14

Noncardiogenic Pulmonary Edema and Diffuse Alveolar Damage

Joseph F. Tomashefski, Jr.

According to the Starling equation, the movement of fluid through a semipermeable membrane is governed by hydrostatic and osmotic pressure gradients and by the intrinsic permeability characteristics of the membrane. Increased pulmonary venous and alveolar capillary hydrostatic pressure are the main determinants of cardiogenic pulmonary edema associated with left ventricular failure or valvular abnormalities (see Chap. 13).

Noncardiogenic pulmonary edema refers to extravascular lung fluid accumulation that is not related to left-sided cardiac dysfunction. Factors that contribute to noncardiogenic pulmonary edema include obstruction of lymphatics or preauricular pulmonary veins, decreased plasma oncotic pressure, and fluid overload. The most important cause of noncardiogenic pulmonary edema is increased permeability of the alveolar capillary membrane occurring in the absence of excessive vascular pressure gradients (*i.e.*, permeability pulmonary edema).

Permeability pulmonary edema is an integral component of acute respiratory failure after severe alveolar injury. The clinical manifestations are stereotypic and have been designated adult respiratory distress syndrome (ARDS).[1] The pulmonary pathologic features of ARDS extend beyond edema to include inflammation, cellular proliferation, and fibrosis. This sequential evolution of lung injury and repair is called diffuse alveolar damage (DAD).[2]

In this chapter, the pulmonary pathologic features of DAD seen in patients with ARDS are correlated with the clinical findings, prognosis, and proposed mechanisms of injury. Other syndromes and causes of noncardiogenic pulmonary edema that mimic ARDS clinically are discussed, and their pathogenesis and pathologic features are contrasted with those of DAD.

ADULT RESPIRATORY DISTRESS SYNDROME AND DIFFUSE ALVEOLAR DAMAGE

The concept of ARDS was first proposed by Ashbaugh and colleagues in 1968 to designate catastrophic respiratory failure, often in previously healthy persons.[1] The syndrome is characterized by dyspnea, progressive hypoxemia, bilateral radiographic lung infiltrates, and decreased pulmonary compliance. Affected patients usually require mechanical ventilatory support, increased concentrations of inspired oxygen (FIO_2), and positive end-expiratory pressure (PEEP). ARDS annually afflicts approximately 150,000 persons in the United States, and despite advances in medical intensive care, the mortality rate remains between 50% and 60%.

Historical Perspective

Pulmonary edema and atelectasis after battlefield trauma were recognized in the trenches of World War I. During World War II, Burford and Burbank designated pulmonary edema after thoracic injury as "traumatic wet lung."[3] In the Vietnam War, the syndrome was fully studied as severely injured soldiers were for the first time resuscitated on the battlefield and quickly evacuated to regional hospitals, where they were stabilized in modern intensive care units.

In the civilian population, a similar syndrome of respiratory failure had been associated with shock and trauma. In a detailed pathologic study of secondary shock published in 1948, Moon described pulmonary hyperemia, edema, hemorrhage, and atelectasis.[4] He astutely suggested endothelial injury as the cause. In

1950, Jenkins and associates reported the clinical details of "congestive atelectasis" and considered overhydration to be the major etiologic factor.[5]

In 1968, Ashbaugh and colleagues emphasized the uniform clinical presentation of respiratory failure in 12 patients after trauma, shock, pancreatitis, or viral infection.[1] The presence of hyaline membranes observed in the lung at autopsy was reminiscent of the neonatal respiratory distress syndrome and suggested to these researchers that surfactant abnormalities were important in the pathogenesis of ARDS.[1]

At approximately the same time, Nash and colleagues elaborated similar pathologic features of lung injury in mechanically ventilated patients and emphasized oxygen toxicity as the most important factor.[6] The controversy over the relative importance of the initial injury compared with the effects of therapy in producing the pulmonary lesions of ARDS remains unresolved.

The term DAD was coined by Katzenstein and colleagues to encompass the stereotypic pulmonary histologic changes seen in ARDS.[2] Bachofen and Weibel, in a landmark article in 1977, described the quantitative ultrastructural features of the lung after septicemic shock.[7]

A detailed quantitative analysis of the histologic features of ARDS was undertaken by Pratt and associates in a multihospital study of patients treated with extracorporeal membrane oxygenation.[8] The importance of pulmonary vascular abnormalities as both cause and effect in ARDS has been stressed by Zapol and associates.[9]

During the past 20 years, there have been intensive efforts in clinical and basic research on ARDS supported by the National Institutes of Health. This effort has expanded the understanding of the natural history, epidemiology, and pathogenesis of this devastating form of acute lung injury.

Causes

A list of the most important causes or conditions associated with ARDS and DAD is presented in Display 14-1. Respiratory failure can be initiated by direct, usually airborne lung injury, as in gastric acid aspirations, pneumonia, or toxic fume inhalation. Frequently, the syndrome is a secondary or bloodborne complication of septicemia, shock, or extrathoracic trauma.[10] Septicemia, especially caused by gram-negative bacteria, is the most important cause of ARDS in the general hospital setting. The mortality of sepsis-induced ARDS approaches 90% in some series. Septicemia is an important factor in ARDS associated with other conditions like trauma, burns, and near-drowning.

ARDS due to primary lung infection is usually the result of viral pneumonia. Bacterial pneumonia can initiate ARDS directly through diffuse lung involvement or indirectly through the mechanism of septicemia. Bacterial pneumonia is an important and frequent complication of ARDS. *Pneumocystis carinii* is another significant cause of ARDS in immunosuppressed patients, including those with the acquired immunodeficiency syndrome.

Because of the stereotypic clinicopathologic features of ARDS, determination of the proximate cause mandates close correlation of clinical and histologic details. The clinical course is frequently obscured by secondary events such as septicemia, oxygen toxicity, and disseminated intravascular coagulation (DIC), which can produce histologic changes resembling those of the original insult. Histologic sampling of the lung should include sites correspond-

---

DISPLAY 14-1. MAJOR CAUSES OF ADULT RESPIRATORY DISTRESS SYNDROME AND DIFFUSE ALVEOLAR DAMAGE

Hematogenous Sources of Lung Injury

Sepsis*

Trauma*

Shock (all causes)*

Drugs or ingested toxins (*e.g.*, narcotics, chemotherapy agents)

Fat embolism

Amniotic fluid embolism

Pancreatitis

Multiple transfusions (*e.g.*, microemboli, leukoagglutinin reactions)

Disseminated intravascular coagulation

Surface burns

Miliary tuberculosis

Thrombotic thrombocytopenic purpura

Leukemia

Paraquat

Cardiopulmonary bypass

Inhalational Sources of Lung Injury

Aspiration of gastric contents*

Diffuse infectious pneumonia (*e.g.*, viral, *Mycoplasma*, *Pneumocystis carinii*, pneumococcal, *Legionella*)*

Near-drowning*

Oxygen toxicity

Irritant gases (*e.g.*, NO_2, Cl_2, SO_2, NH_3, phosgene, cadmium)

Smoke inhalation

Direct Physical Lung Injury

Lung contusion

Irradiation

* *Most important causes of adult respiratory distress syndrome.*

Adapted from Hudson LD. Causes of the adult respiratory distress syndrome—clinical recognition. Clin Chest Med 1982;3:195.

---

ing to the initial radiographic infiltrates. Lung tissue in suspected cases of ARDS should, when indicated, be cultured for respiratory viruses in addition to routine evaluation for bacteria and fungi. Except for cases of known or suspected autoimmune disease, immunofluorescence staining of the lung tissue is of little value. Electron microscopic evaluation rarely elucidates an underlying cause. In some patients, all efforts fail to reveal a convincing etiologic factor.

Clinical and Radiographic Features

During the first 12 to 24 hours after injury, the patient appears stable, with few pulmonary signs or symptoms and minimal findings on the chest radiograph. If ARDS is caused by pneumonia or acid aspiration, there may be a localized radiographic infiltrate. The earliest clinical sign is tachypnea associated with hypoxemia that is not corrected by increasing the FIO_2. Between 1 and 5 days after the onset of symptoms, crackles are audible, and bilateral alveolar infiltrates with air bronchograms appear on chest x-ray films (Fig. 14-1). Computed tomography scans frequently demonstrate that lung consolidation is irregularly distributed or gravitationally dependent, even when the infiltrates on the chest
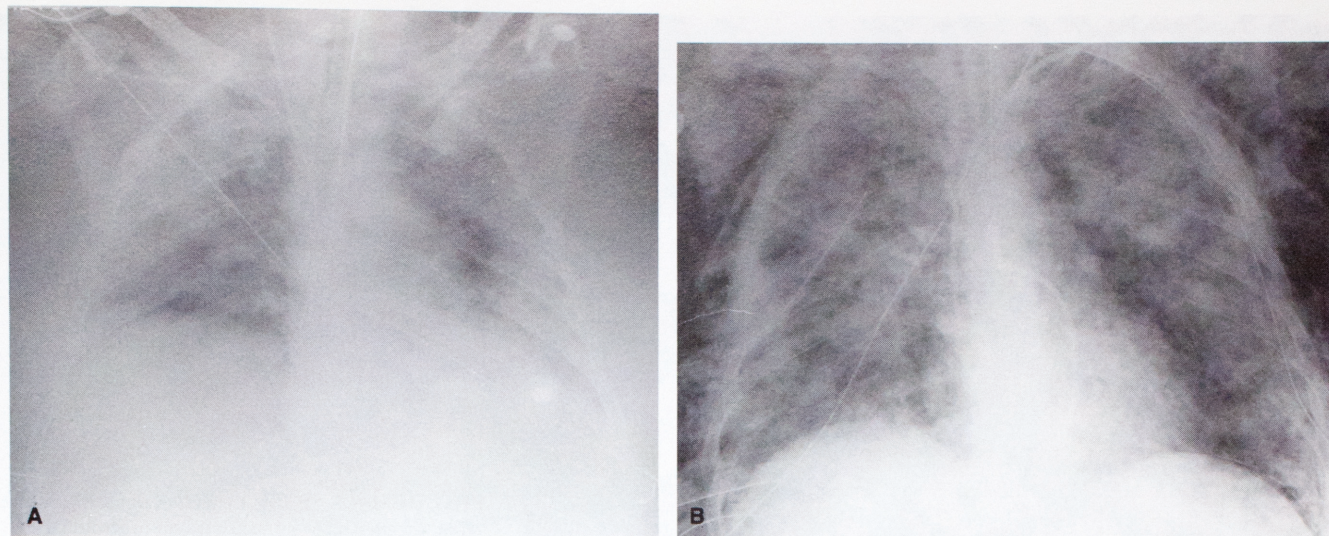
FIGURE 14-1. (**A**) In early adult respiratory distress syndrome caused by septicemia, diffuse bilateral alveolar infiltrates obscure the left heart border and diaphragm. (**B**) In the same patient after 23 days of mechanical ventilation and positive end-expiratory pressure, coarse reticulonodular infiltrates and extensive subcutaneous emphysema are present.

radiograph appear diffuse (Fig. 14-2).[11] Patients usually require mechanical ventilation with supplemental oxygen and PEEP. The clinical presentation mimics that of congestive heart failure, which is excluded by a pulmonary capillary wedge pressure within the normal range (<15 mm Hg).

Between 3 and 7 days from the onset of symptoms, radiographic consolidation becomes less confluent and ground-glass infiltrates emerge as the lung is transformed from an edematous to a fibrotic organ. The lungs are stiff, and pulmonary artery pressure may be elevated. Patients are at constant risk of ventilator-associated barotrauma resulting in pneumothorax, pneumomediastinum, and subcutaneous emphysema. Pulmonary superinfection and multiorgan failure are frequent complications of ARDS and often are the cause of death.

## PULMONARY PATHOLOGY OF DIFFUSE ALVEOLAR DAMAGE

The pathologic features of the lung in ARDS represent a time-dependent, stereotypic response to alveolar injury.[2] DAD can be conveniently divided into three sequential and overlapping phases: the exudative phase of edema and hemorrhage, the proliferative phase of organization and repair, and the fibrotic phase of end-stage fibrosis. The patient's histologic features correlate more with the duration of injury than its initiating cause. Permeability pulmonary edema, a signal feature of acute alveolar injury, is prominent in the early stages and heralds the onset of rapidly progressive pulmonary fibrosis, which dominates the later course of the disease and is often a limiting factor for survival.

Exudative Phase

The exudative phase of DAD comprises the first 4 to 7 days after the onset of respiratory failure. The lungs of patients who die during this period are heavy, and the visceral pleura is red-blue and focally hemorrhagic. The parenchymal surface is dark red with a

diffuse, airless consistency and, on compression, exudes small amounts of hemorrhagic fluid (Color Fig. 14-1). Close inspection of the formalin-inflated specimen reveals punctate air spaces that represent dilated alveolar ducts accentuated by adjacent collapsed or indurated parenchyma. In patients who die of severe respiratory failure, the lungs are usually diffusely involved, but the process may be regionally distributed.[12]

The earliest histologic changes are pulmonary capillary congestion and interstitial and alveolar edema. The most distinctive feature of the exudative phase is eosinophilic hyaline membranes, which develop soon after the initial injury. Hyaline membranes are concentrated along the alveolar duct, where they adhere to the tips of alveolar septa and extend across the alveolar orifices (Fig. 14-3). Hyaline membranes are composed of fibrin and serum proteins that have leaked through the injured alveolocapillary membrane and mixed with cellular debris within the alveolar space. Immunohistochemical and immunofluorescent staining demonstrates fibrinogen, immunoglobulin, and complement within the hyaline membrane and a thin layer of fibronectin on its surface. Alveolar
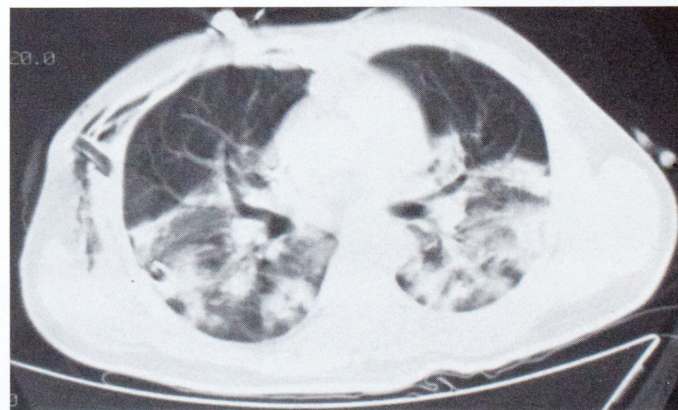
FIGURE 14-2. A CT scan reveals adult respiratory distress syndrome after myocardial infarction and cardiopulmonary bypass. Confluent infiltrates are localized in the posterior, dependent regions.
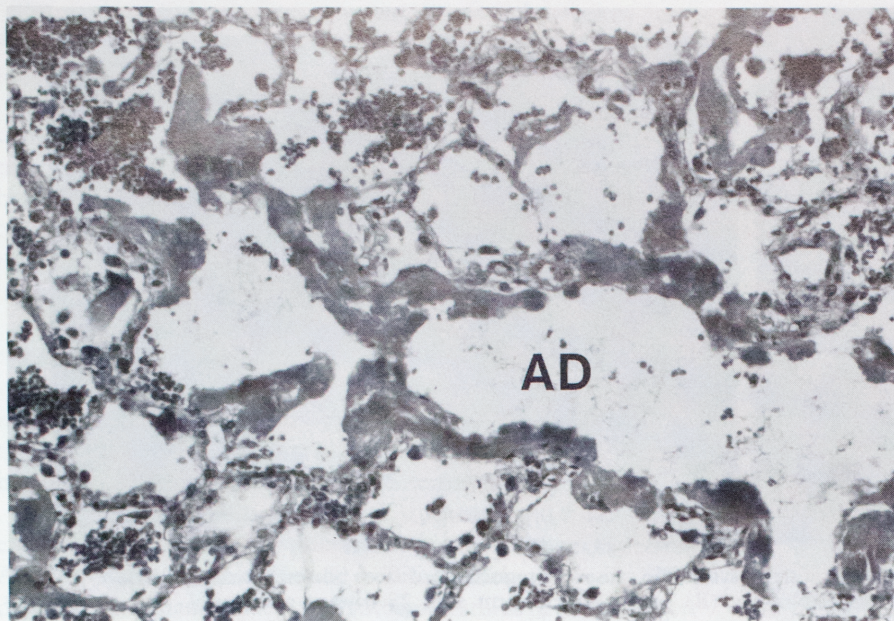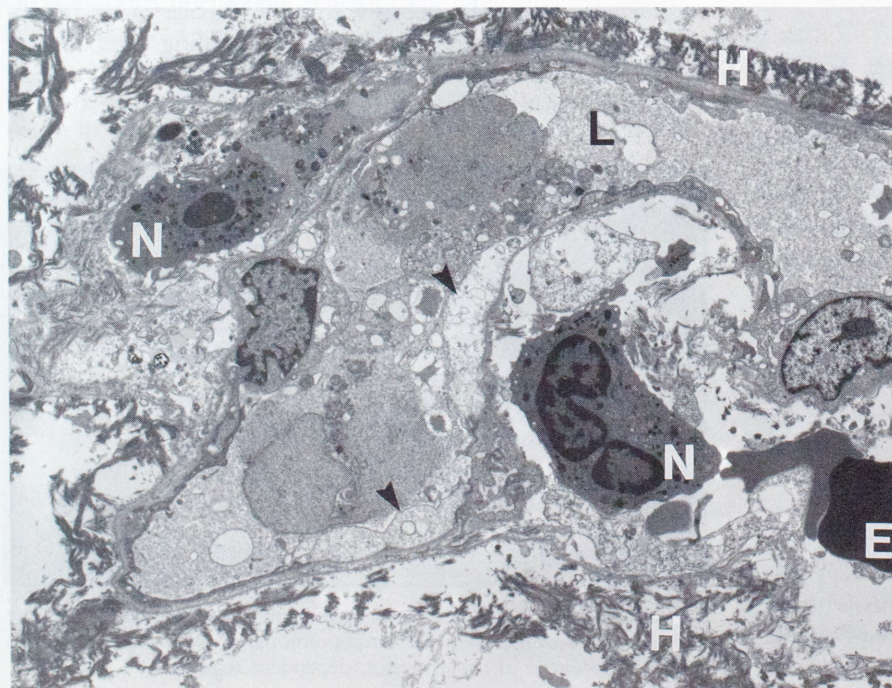
FIGURE 14-3. In the exudative phase of diffuse alveolar damage, coarse hyaline membranes line the alveolar duct (AD) and traverse the alveolar orifices. Notice the acute alveolar hemorrhage and alveolar septal edema. (H & E stain; low magnification.)

ducts appear dilated unlike the adjacent alveoli, which are collapsed, congested, and partly filled with fibrinous exudate (see Fig. 14-3). Periductal atelectasis is partly ascribed to acquired abnormalities of surfactant and consequent elevation of alveolar surface tension.

Ultrastructurally, hyaline membranes are layered on a denuded alveolar basement membrane (Fig. 14-4). There is evidence of injury to capillary endothelial and alveolar epithelial cells, but the epithelial damage is usually more pronounced. Endothelial abnormalities include increased pinocytotic vesicles, cytoplasmic swelling, and separation of the endothelial junctions. Occasionally, endothelial necrosis and intracapillary fibrin thrombi are seen (Fig. 14-5). Relatively subtle endothelial changes may underlie significant functional impairment. Bachofen and Weibel have suggested that the remarkable reparative capability of endothelial cells masks transient endothelial lesions.[7] Neutrophils are aggregated in alveolar capillaries and are sparsely distributed in the interstitium and alveolar spaces.

The alveolar septa are greatly expanded by edema, fibrin, and extravasated erythrocytes, providing evidence of increased capillary permeability (see Fig. 14-5). Regardless of whether the initiating cause of ARDS is airborne or bloodborne, there is extensive necrosis of type 1 alveolar epithelial cells, which slough from the alveolar basement membrane (see Figs. 14-4 and 14-5). Type 2 cells, which are more resistant to injury, persist and have the capacity to differentiate into type 1 cells. Quantitative ultrastructural studies of the early phase of DAD document an increased volume of the interstitial compartment due to interstitial edema.

FIGURE 14-4. In the exudative phase of diffuse alveolar damage, fibrinous hyaline membranes (H) are layered on a denuded alveolar basement membrane. The alveolar wall is edematous, with extravascular neutrophils (N) and erythrocytes (E). Capillary endothelial cells (*arrowheads*) are swollen. The capillary lumen (L) contains cellular debris. (Original magnification × 3075.)
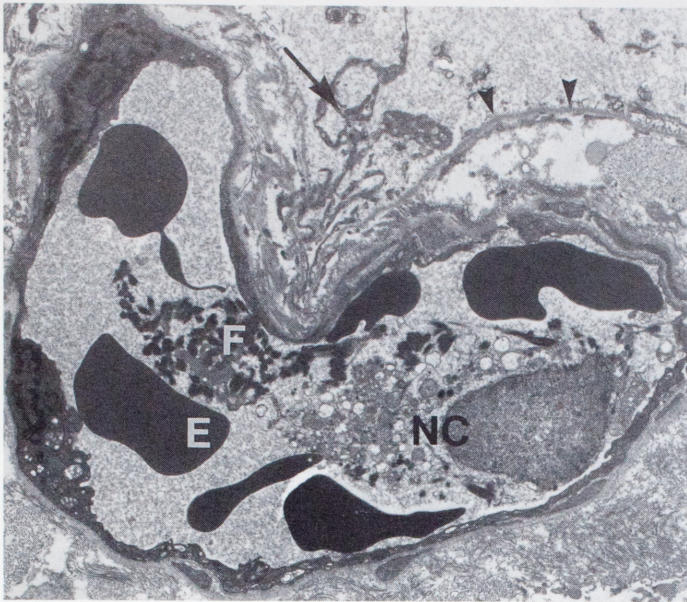
FIGURE 14-5. In the exudative phase of diffuse alveolar damage, the capillary contains erythrocytes (E), fibrin strands (F), and necrotic cells (NC). The alveolar epithelial surface is denuded (*arrowheads*). Necrotic remnants of type 1 cells (*arrow*) have sloughed from the basement membrane. (Original magnification × 4950.)

This is accompanied by a reduced volume density of alveolar epithelium and alveolar capillaries. The volume density of intracapillary granulocytes is increased.[7,12]

Proliferative Phase

In the proliferative phase of DAD, permeability pulmonary edema is overshadowed by organization, inflammation, and fibrosis. The lungs of patients who die between 1 and 3 weeks after the onset of respiratory failure often exceed 2000 g in combined weight and are rigid and pale red (Fig. 14-6). The parenchymal surface is glistening, with a slippery texture due to the presence of newly formed connective tissue. Zones of complete air-space effacement

alternate with areas in which dilated air spaces, 1 to 2 mm in diameter, are accentuated by adjacent fibrous tissue (see Fig. 14-6).

The histology of the proliferative phase is dominated by hyperplastic type 2 pneumocytes that line the alveolar surface (Fig. 14-7). Alveolar walls are widened by activated mesenchymal cells, chronic inflammation, and fibromyxoid tissue that stains positively with Alcian blue because of abundant mucopolysaccharides. Type 2 pneumocytes have large, hyperchromatic nuclei, prominent nucleoli, and various degrees of nuclear atypia (Fig. 14-8). Nuclear atypia is most extreme in lung injury induced by irradiation, antineoplastic chemotherapy, and viral infection, but atypia may be severe even in the absence of these factors.

Ultrastructurally, proliferating pneumocytes contain cytoplasmic lamellar bodies and surface microvilli (see Fig. 14-8). Immunohistochemically, these cells stain for surfactant apoprotein, indicative of type 2 cell differentiation. Lamellar bodies may be abnormally large and complex and their density low. Transition forms between type 1 and 2 pneumocytes are represented as elongated cells with short microvilli and rare lamellar bodies. Squamous metaplasia is prominent in bronchioles and alveoli, and cytoplasmic hyaline, a nonspecific marker of cell injury, can be seen in cells expressing squamous differentiation.[12] In cytologic smears of bronchial washings, atypical pneumocytes or metaplastic squamous epithelium can be mistaken for carcinoma. Epithelial hyperplasia is accompanied by the proliferation of mesenchymal cells, which are responsible for the fibrous reorganization of the lung. Fibroblasts and myofibroblasts proliferate within the alveolar wall, align themselves parallel to the alveolar surface, and migrate through gaps in the basement membrane into the alveolar space, where they convert fibrinous exudate into collagen (Fig. 14-9).[13] Intraluminal fibrosis by accretion occurs from the respiratory bronchiole to the alveolus, but it is more pronounced in the alveolar duct, where it was designated "alveolar duct fibrosis" by Pratt and colleagues (Fig. 14-10).[8]

Although alveolar septal fibrosis contributes to lung remodeling, intraluminal fibrosis is emphasized as the most important mechanism of fibroplasia in ARDS.[13] Within the alveolar duct, organizing granulation tissue can assume several patterns (see Fig. 14-10). Fibrous tissue can occlude the lumen of the duct or be
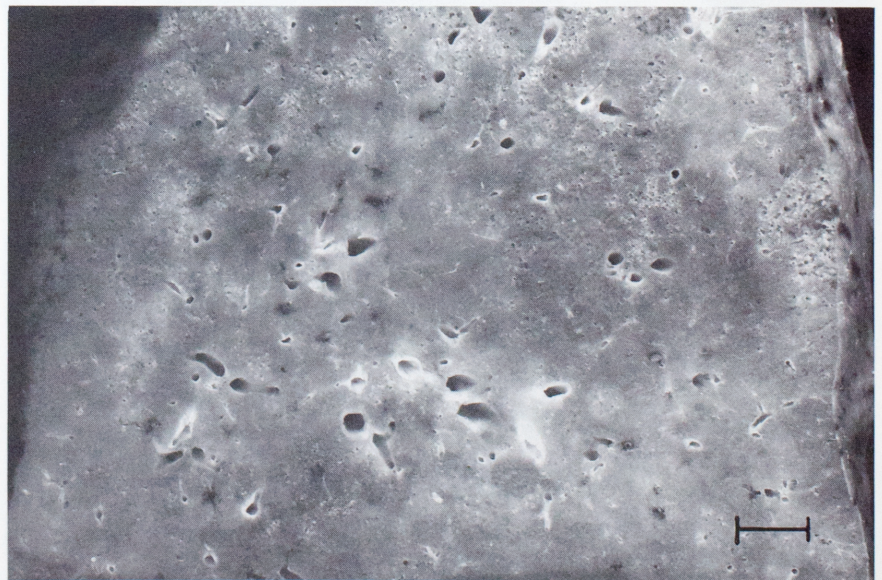
FIGURE 14-6. In the proliferative phase of diffuse alveolar damage, pale fibrous effacement alternates with areas in which airspaces are preserved. (Scale = 0.8 cm).
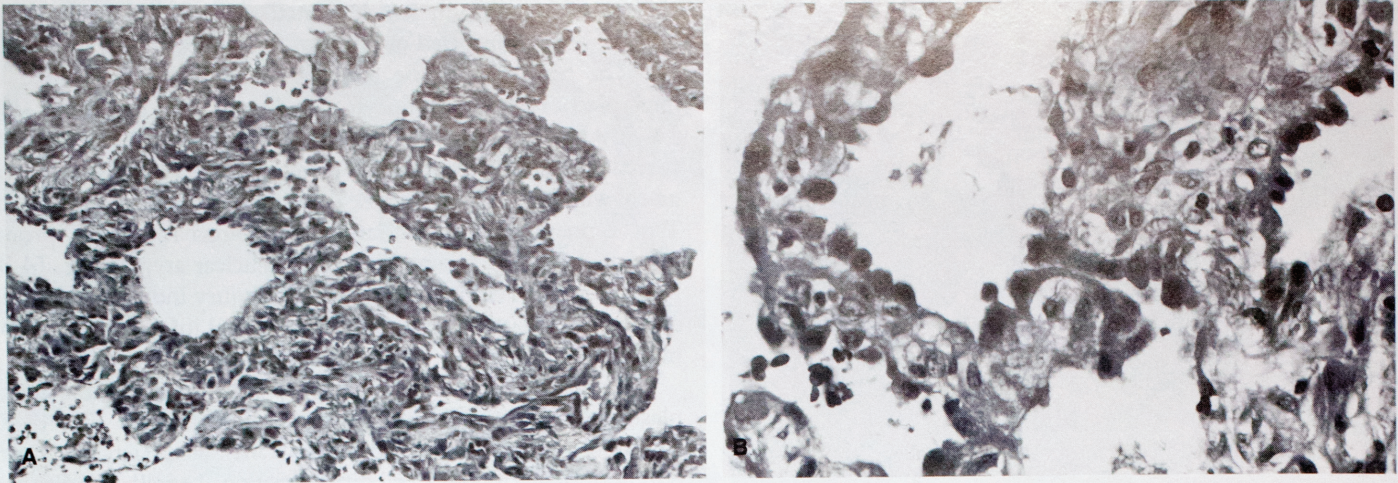
FIGURE 14-7. (**A**) In the proliferative phase of diffuse alveolar damage, there is coarse alveoloseptal remodeling by extensive mesenchymal cell proliferation. (H & E stain; low magnification.) (**B**) Alveolar septa are widened by edema, connective tissue, and reactive mesenchymal cells. The alveolar surface is partially covered by hyperplastic type 2 pneumocytes. (H & E stain; intermediate magnification.)

distributed peripherally within the duct as a fibrous ring. When filled with neutrophils or erythrocytes, ringlike alveolar duct fibrosis can be misinterpreted histologically for microabscesses or vascular malformations.[8,12] As organization progresses, alveolar pneumocytes proliferate over the surface and incorporate the intraluminal exudate into the interstitium.

After injury to the alveolocapillary unit, alveolar septa collapse and become sealed in apposition by organizing fibrin and proliferating pneumocytes.[12] This collapse induration is another mechanism of alveolar remodeling that is best observed ultrastructurally as deep folds of the alveolar basement membrane traversed by type 2 pneumocytes (see Fig. 14-8). Distorted remnants of basement membrane material may be observed in the thickened alveolar wall.

Morphometric studies of the lung in the proliferative phase indicate an increased volume proportion of the epithelial layer due to regeneration of type 2 cells.[7,12] The decreased volume density of capillaries persists and is associated with an increase in interstitial fibroblasts. Using light microscopic morphometry, Fukuda and colleagues demonstrated a gradual increase in the percentage of interstitial tissue with increased duration of ARDS.[13] The percentage of lung parenchyma involved by intraalveolar fibrosis was increased beyond 10 days, but by day 35, the distinction between intraalveolar and interstitial fibrosis was no longer possible because of extensive fibrous remodeling.

Fibrotic Phase and Long-Standing, Healed Adult Respiratory Distress Syndrome

Within 3 to 4 weeks of the onset of ARDS, the lung is completely remodeled by sparsely cellular collagenous tissue. The visceral pleura is coarsely nodular, and the parenchyma demonstrates dif-
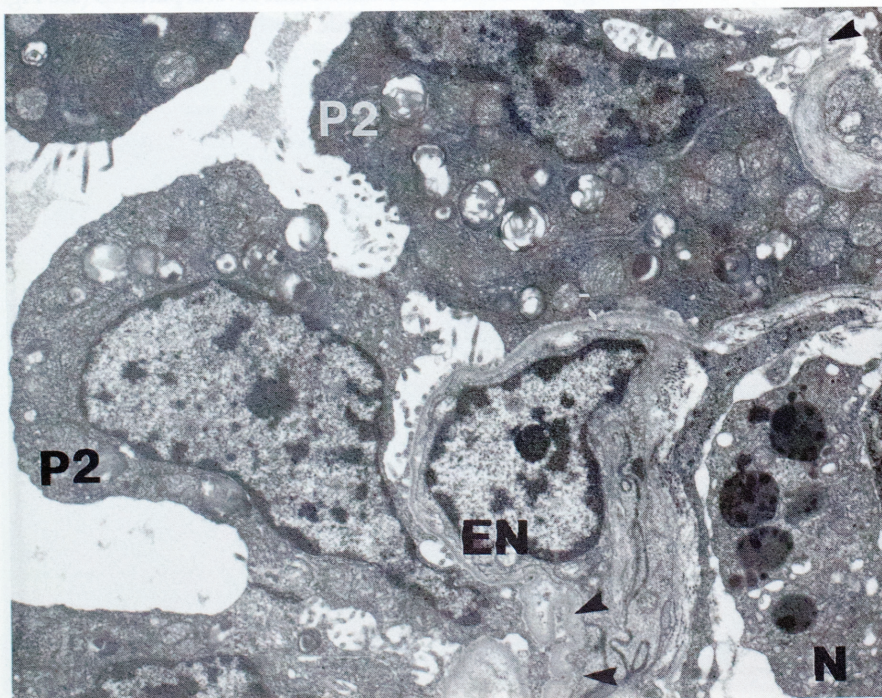
FIGURE 14-8. Type 2 pneumocytes (P2) are characterized by cytoplasmic lamellar bodies and microvilli. The alveolar basement membrane is infolded (*arrowheads*), and a swollen endothelial cell (EN) occupies the lumen of a capillary. A neutrophil (N) is in the interstitium. (Original magnification × 7600.)
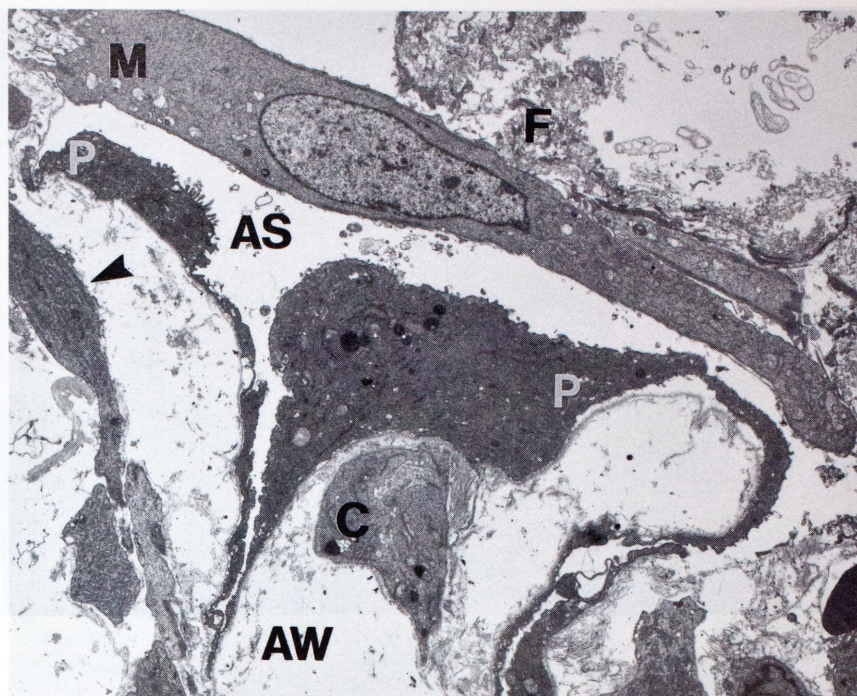
FIGURE 14-9. Massively edematous alveolar wall (AW) is focally lined by cells showing transitional features between type 1 and type 2 pneumocytes (P). A primitive mesenchymal cell (M) has entered the alveolar space (AS) and is in contact with the fibrinous exudate (F). Another mesenchymal cell (*arrowhead*) is aligned parallel to the basement membrane. An alveolar capillary (C) contains prominent endothelial cells. The distance between the capillary and alveolar basement membrane is increased. (Original magnification × 3075.)

fuse fibrosis or pale irregular scars alternating with microcystic air spaces, 1 mm or larger in diameter (Fig. 14-11). The formation of contiguous large cysts (*i.e.*, adult bronchopulmonary dysplasia) is unusual.[14] Large cystic spaces may result from healed abscesses, emphysematous bullae, or persistent interstitial emphysema. Peripheral bronchi are dilated and abnormally approach the pleura (see Fig. 14-11). Microscopically, alveolar septa are widened by collagen. Thick fibrous cords or stellate scars occur in distorted, dilated remnants of alveolar ducts. Fibrotic microcysts represent progression of ring-shaped alveolar duct fibrosis. Honeycombing focally resembles that seen in idiopathic pulmonary fibrosis, but the size of the air spaces is generally smaller (Fig. 14-12). The total lung collagen is increased in patients who survive more than 14 days, and the concentration and total amount of collagen have been correlated with the extent of fibrosis assessed histologically.[15]

Long-term follow-up studies of patients who survive an episode of ARDS indicate that approximately two thirds have abnormal pulmonary function tests 1 year later. Severe pulmonary dysfunction persists in only a few survivors. Prolonged pulmonary disability has been correlated with the initial severity of lung impairment or the persistence of lung impairment during the acute episode but not with the histologic features seen on open lung biopsy.[16,17] The phenomenon of long-term survivors with moderate or good pulmonary function, who during their episode of ARDS demonstrated extensive fibrosis on open lung biopsy, has suggested that fibrosis observed early in ARDS is potentially
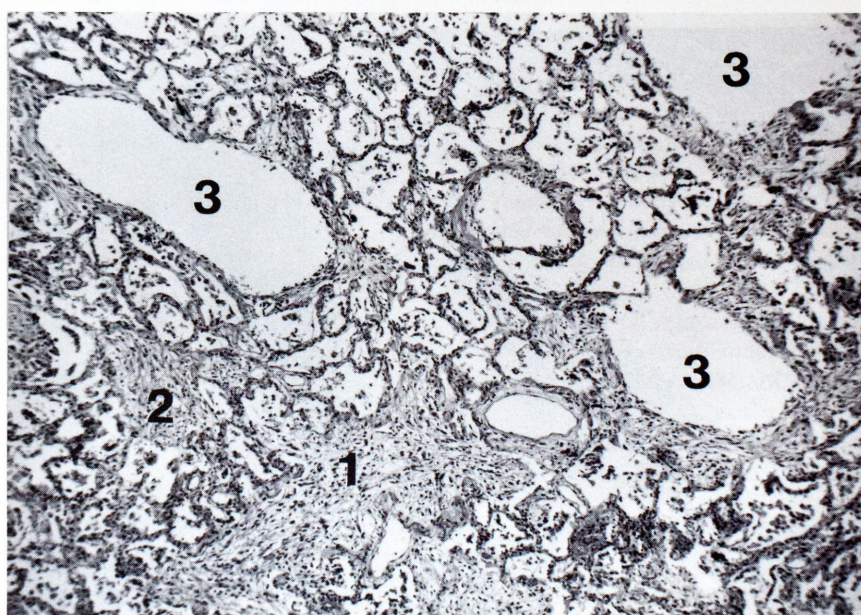
FIGURE 14-10. Patterns of alveolar duct fibrosis. Occlusions of alveolar duct lumens by plugs of granulation tissue are seen in longitudinal (1) and cross-section (2) samples. The peripheral orientation of fibrous tissue in the alveolar duct produces microcysts (3). (H & E stain; low magnification; from Tomashefski JF Jr. Pulmonary pathology of the adult respiratory distress syndrome. Clin Chest Med 1990;11:593.)
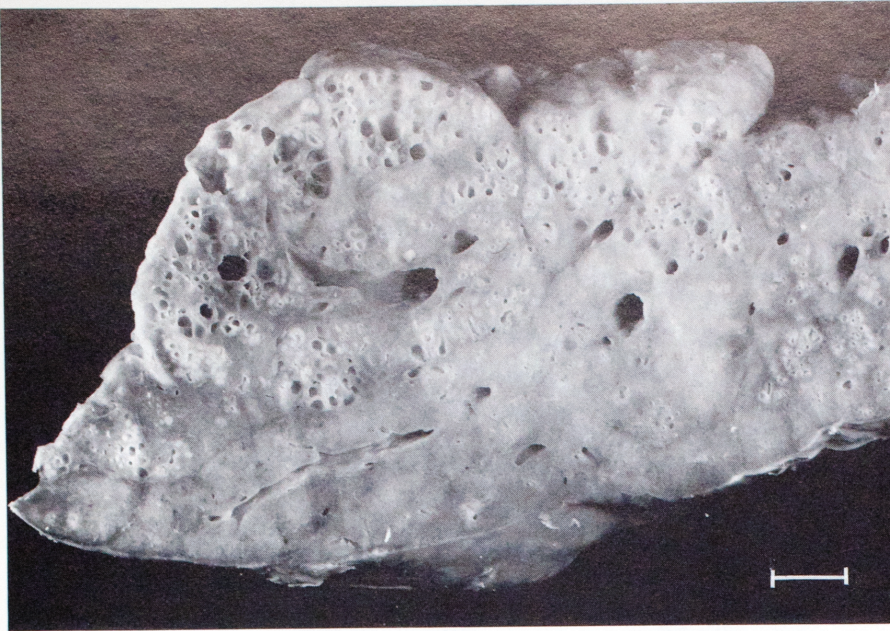
FIGURE 14-11. In the fibrotic phase of diffuse alveolar damage, areas of diffuse fibrosis (*bottom*) alternate with microcystic honeycombing. The airways are abnormally close to the pleural surface. (Scale = 2 cm.)

reversible.[17,18] However, it is more likely that this discrepancy is due to sampling of regionally distributed DAD at the time of open lung biopsy.

There have been few studies of lung morphology in survivors of ARDS. Lakshminarayan and colleagues observed mild interstitial fibrosis, epithelial hyperplasia, and increased alveolar macrophages with interstitial lymphocytes in a patient 9 months after ARDS.[16] Pratt found bundles of collagen within alveolar ducts of a patient successfully weaned from the ventilator.[19] In a personally studied case, severe obliterative alveolar duct fibrosis persisted in a patient who survived 2 months after having been weaned from the ventilator after ARDS probably caused by a viral infection. The factors that account for survival in ARDS and the degree and mechanisms of resolution of fibrosis are poorly understood.

Pulmonary Vascular Remodeling

Pulmonary hypertension is an important complication of ARDS, and lung vascular changes follow a temporal sequence that correlates with the duration of alveolar damage.[20] Vascular injection studies using silicone polymer or barium sulfate gelatin demonstrate markedly reduced vascular filling of postmortem lung specimens (Fig. 14-13).[9,20] Early in the course of ARDS vasoconstriction, interstitial edema or thromboembolism may contribute to a raised pulmonary artery pressure. After several weeks, fibrous obliteration of the microcirculation and increased arterial muscularization are fixed lesions that account for increased pulmonary vascular resistance.

Thromboemboli have been documented by vascular injection studies in 95% of lungs examined at autopsy. Macrothrombi in
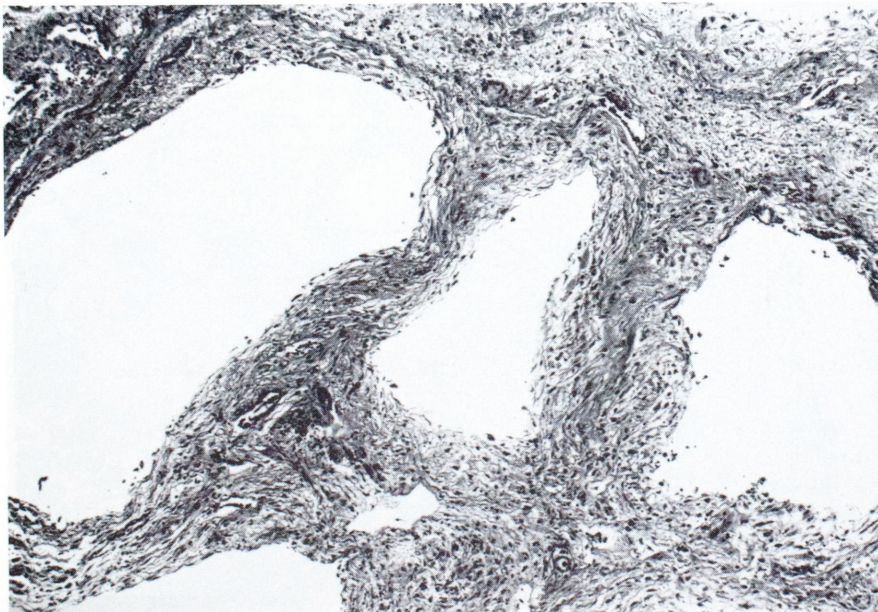
FIGURE 14-12. Enlarged, fibrous-walled air spaces are arranged in a honeycomb pattern in the same patient as that in Fig. 14-11. (Movat pentachrome stain; low magnification.)
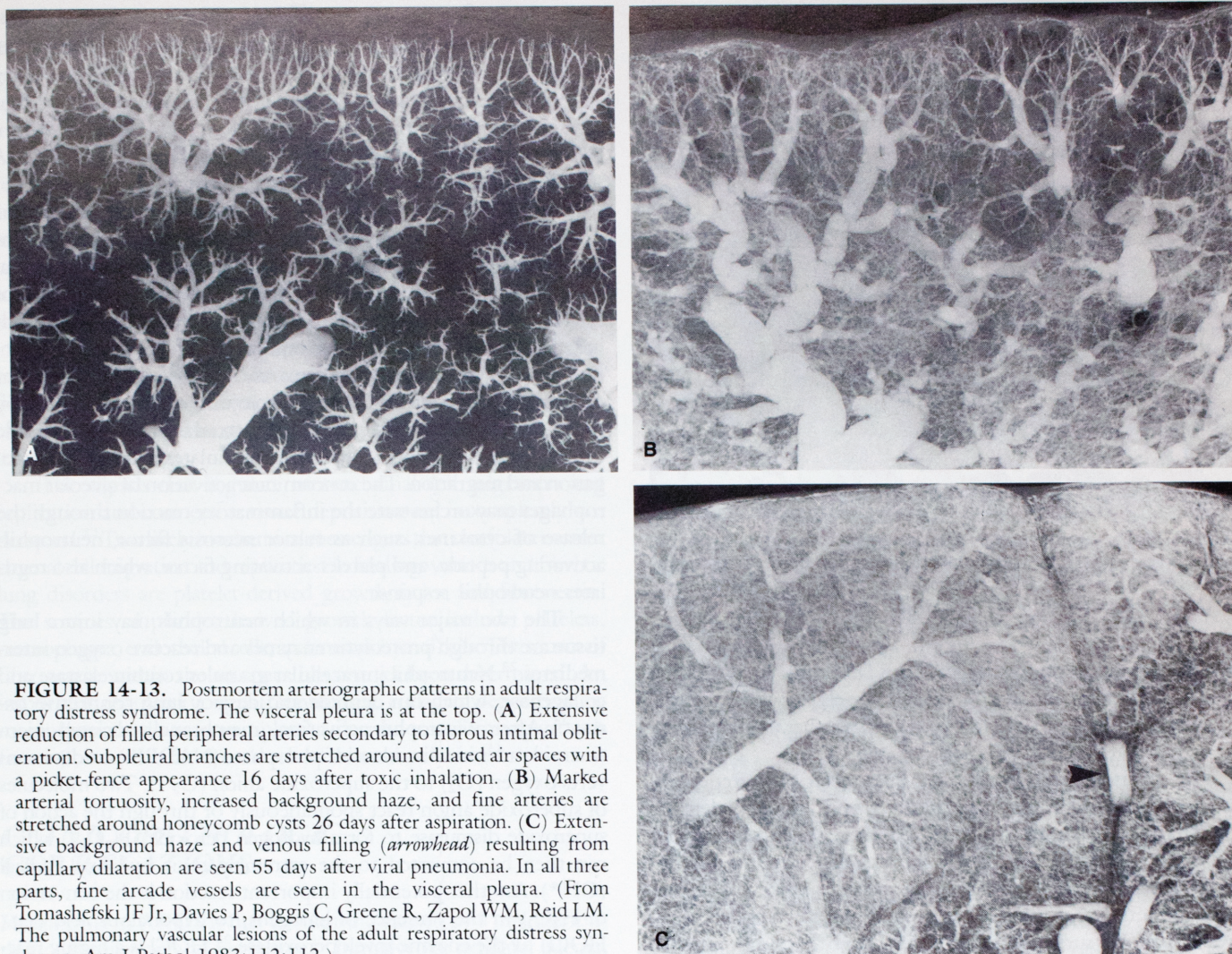
FIGURE 14-13. Postmortem arteriographic patterns in adult respiratory distress syndrome. The visceral pleura is at the top. (**A**) Extensive reduction of filled peripheral arteries secondary to fibrous intimal obliteration. Subpleural branches are stretched around dilated air spaces with a picket-fence appearance 16 days after toxic inhalation. (**B**) Marked arterial tortuosity, increased background haze, and fine arteries are stretched around honeycomb cysts 26 days after aspiration. (**C**) Extensive background haze and venous filling (*arrowhead*) resulting from capillary dilatation are seen 55 days after viral pneumonia. In all three parts, fine arcade vessels are seen in the visceral pleura. (From Tomashefski JF Jr, Davies P, Boggis C, Greene R, Zapol WM, Reid LM. The pulmonary vascular lesions of the adult respiratory distress syndrome. Am J Pathol 1983;112:112.)

arteries greater than 1 mm in diameter correspond to the vascular filling defects, which have been demonstrated by bedside balloon occlusion angiography in 48% of patients with ARDS.[12] Microthrombi in arteries less than 1 mm diameter contribute to the generalized decreased vascular filling seen in postmortem arteriograms. Platelet-fibrin thrombi confined to capillaries and small arterioles are most numerous in the exudative phase of DAD and are thought to represent localized intravascular coagulation or DIC (see Fig. 14-5). Larger clots may be embolic or formed *in situ*; morphologically, it is impossible to tell the difference.

Classic, wedge-shaped, hemorrhagic pulmonary infarcts may be seen in DAD, but frequently infarcts assume unusual patterns such as multifocal lobular necrosis or bandlike zones of necrosis subjacent to the visceral pleura.[9,11] Peripheral lung parenchyma is particularly susceptible to ischemic necrosis because of reduced collateral blood flow. Postmortem studies using indocyanine green instilled into the airways indicate preferential ventilation of hypoperfused areas. These peripheral necrotic regions are predisposed to infection and barotrauma, resulting in lung cavitation, pneumothorax, and bronchopleural fistula.[9] Communicating pleural arcade vessels that fill from pulmonary artery to pulmonary artery frequently bridge peripheral hypoperfused areas, but the ability of these arcades to provide collateral blood flow is not determined (see Fig. 14-13).[9,11]

In the proliferative and fibrotic stages of DAD, fibrocellular intimal proliferation is a response to endothelial injury in arteries, veins, and lymphatics. Vascular lumens are narrowed by concentrically layered fibrin, proliferating myointimal cells, hyperplastic endothelial cells, and fibromyxoid connective tissue (Fig. 14-14). Obstruction of veins and lymphatics potentially increases intracapillary pressure, contributing to the accumulation of interstitial edema and impeding the removal of extravascular fluid from the lung.

In the late proliferative and fibrotic stages of DAD, postmortem arteriograms show preacinar arteries stretched about fibrous-walled cysts and dilated air spaces (see Fig. 14-13). Serpentine arterial branches have thickened fibromuscular walls. Arterial tortuosity occurs as a result of distortion by irregularly contracting fibrous tissue. Dilated pulmonary capillaries permit the passage of barium-gelatin injection medium, which is normally restricted to vessels with a diameter greater than 15 μm, through the capillary bed into pulmonary veins. This produces a dense, ground-glass background haze on postmortem arteriograms (see Fig. 14-13). An increased concentration of blood
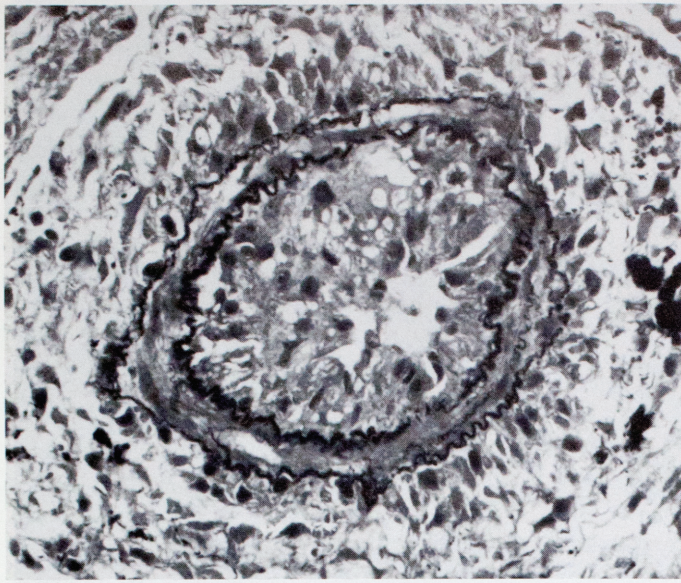
FIGURE 14-14. A muscular pulmonary artery with medial hypertrophy, obliterative endarteritis, perivascular fibrosis, and fibroblast proliferation is seen 17 days after cardiopulmonary bypass and myocardial infarction. (Movat pentachrome stain; intermediate magnification.)

vessels in patients in the last stages of ARDS probably reflects the combined effects of abnormally dilated vessels, crowding of vessels, and increased profiles of tortuous vessels rather than a restoration or regrowth of normal arteries.[20]

Hypermuscularization of pulmonary arteries is frequently associated with pulmonary hypertension and has been demonstrated morphometrically in ARDS.[20] With increasing duration of lung injury, the thickness of the media relative to the arterial diameter increases. The percentage of muscular thickness of preacinar and intraacinar arteries has been shown to be significantly lower in patients surviving fewer than 9 days than in those who survive at least 20 days. The degree of medial thickness of muscular arteries increases with the duration of ARDS. There is evidence of peripheral extension of smooth muscle into normally nonmus-

cularized arteries and arterioles.[20] Potential causes of arterial muscularization in ARDS include hypoxia, pulmonary hypertension, and oxygen toxicity.[9]

PATHOGENESIS OF DIFFUSE ALVEOLAR DAMAGE

The pathogenesis of lung injury in ARDS is complex and incompletely understood.[21,22] The neutrophil has been assigned a pivotal role in initiating the syndrome, but well-documented cases of ARDS in neutropenic patients attest to important neutrophil-independent pathways of lung injury.

One of the most comprehensively studied and most relevant experimental models of acute lung injury is that produced by sepsis or endotoxin (Fig. 14-15).[21] Bacterial lipopolysaccharide directly or by activating complement stimulates neutrophil aggregation and migration. The concomitant activation of alveolar macrophages may orchestrate the inflammatory reaction through the release of cytokines, such as tumor necrosis factor, neutrophil-activating peptide, and platelet-activating factor, which also regulates neutrophil response.

The two major ways in which neutrophils may injure lung tissue are through proteolytic enzymes and reactive oxygen intermediates.[23] Neutrophil intracellular granules contain elastase and collagenase, which can degrade and destroy lung connective tissue.[23] After neutrophil activation, membrane-associated nicotinamide adenine dinucleotide phosphate (NADPH) oxidase converts oxygen (O_2) to the superoxide anion (O_2^-). Two molecules of superoxide anion react spontaneously or through the action of superoxide dismutase to form hydrogen peroxide (H_2O_2), which can then be converted to the extremely toxic hydroxyl radical (OH^*). Another potentially important reaction is the conversion of H_2O_2, in the presence of halogens, to hypohalous acid (e.g., HOCl) by the enzyme myeloperoxidase.[23] HOCl is a highly reactive oxidant that attacks a wide range of biologic molecules, including antiproteases, indirectly facilitating proteolytic lung destruction.
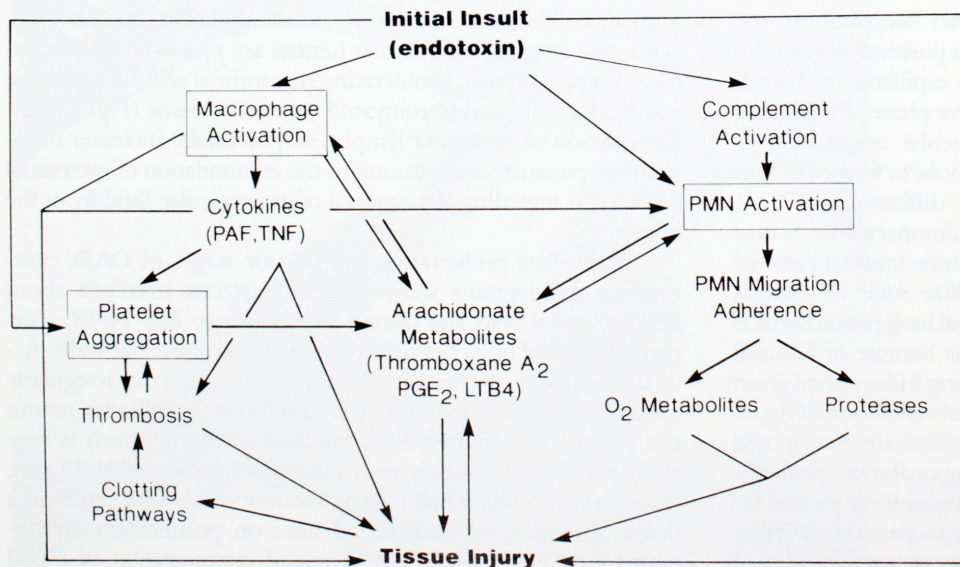
FIGURE 14-15. The proposed pathways of lung injury in adult respiratory distress syndrome due to septicemia are intertwined. (LTB4, leukotriene B4; PAF, platelet activating factor; PGE$_2$, prostaglandin E$_2$; PMN, polymorphonuclear leukocyte; TNF, tumor necrosis factor.)

CHAPTER 14: Noncardiogenic Pulmonary Edema and Diffuse Alveolar Damage 135

Metabolites of arachidonic acid such as thromboxane A_2 and leukotriene B_4 are produced, respectively, through the cyclooxygenase or lipoxygenase pathways after generation of arachidonic acid by phospholipase. These potent vasoactive mediators were initially thought to be the final common pathway of lung injury in ARDS, but they are now considered to be a nonspecific result of cell membrane injury and neutrophil activation.[21] Metabolites of arachidonic acid may be important in the regulation of the inflammatory response.

Disordered blood coagulation, including acute DIC, frequently accompanies and possibly initiates ARDS. Clots are often present in lung vessels, and endothelial injury is considered to be an important cause of *in situ* pulmonary thrombosis. Experimentally, particulate and soluble products of intravascular coagulation and fibrinolysis cause pulmonary microvascular injury.[9,20] Whether embolic or produced *in situ*, pulmonary thrombi exacerbate lung injury and necrosis.

The signals that regulate mesenchymal cell migration and replication and connective tissue deposition are incompletely understood.[22] Two likely biochemical messengers that modulate mesenchymal cell migration and replication in healing wounds and fibrotic lung disorders are platelet-derived growth factor and fibronectin. The sources of platelet-derived growth factor include platelets, macrophages, endothelial cells, and mesenchymal cells. The source of fibronectin within the air space has not yet been determined. An important regulatory signal controlling collagen deposition by mesenchymal cells *in vitro* is platelet-derived transforming growth factor-β, which is in the alveoli of normal persons.[22]

CLINICOPATHOLOGIC CORRELATIONS

Hypoxemia in ARDS is due to shunting caused by a maldistribution of ventilation and perfusion.[12] Intraalveolar exudate, edema, fibrosis, and atelectasis contribute to shunting. Lamy and associates correlated the histologic features on open lung biopsy with physiologic parameters in three subgroups of patients with ARDS.[18] Group 1 patients had a fixed shunt resistant to increasing F_{IO_2} and minimal response to PEEP. Lung biopsies demonstrated alveoli filled with edema, hemorrhage, and exudate. Patients in group 2, who had hypoxemia, a shunt that worsened with decreasing F_{IO_2}, and a moderately slow response to PEEP, had extensive fibrosis on open lung biopsy. Survival was best in group 3 patients, with less severe hypoxemia, a shunt that worsened with decreasing F_{IO_2}, and a prompt, significant increase in arterial oxygenation with PEEP. Lung biopsy specimens in this group showed less extensive intraalveolar exudate and atelectasis, with many open alveoli allowing gas exchange. Another potential mechanism of hypoxemia in ARDS is impaired diffusion of oxygen due to alveolar septal fibrosis and a thickened epithelial layer of type 2 pneumocytes.[7]

Obliterative pulmonary vascular lesions in ARDS result in pulmonary hypertension and account for an increased physiologic dead space secondary to the ventilation of poorly perfused areas of the lung. Vasoconstriction caused by hypoxia contributes to increased vascular resistance. Increased dead space and pulmonary hypertension are more severe in the late stages of ARDS. Lung compliance is lowered by interstitial edema, atelectasis, and inflammatory exudate in the early stages of ARDS. In the last stages, compliance is reduced by extensive fibrosis.

DIFFERENTIAL DIAGNOSIS OF DIFFUSE ALVEOLAR DAMAGE

The histologic differential diagnosis of DAD includes infantile hyaline membrane disease (IHMD), acute bacterial pneumonia, bronchiolitis obliterans organizing pneumonia (BOOP), and usual interstitial pneumonia (UIP). The differentiation of IHMD from the exudative phase of DAD is based exclusively on the clinical setting and immaturity of the affected lung in IHMD. In the full-term neonate and older child, ARDS is clinically and histologically similar to the syndrome in the adult. Specific causes of DAD in the neonate, such as meconium aspiration or streptococcal or viral pneumonia, may be suggested by the respective findings of amniotic debris, hyaline membranes impregnated by bacteria, or viral inclusions (see Chap. 11).

In acute bronchopneumonia, hyaline membranes and edema may be focally distributed with the acute inflammatory exudate. The term DAD is reserved for generalized distribution of histologic lesions beyond the immediate areas of acute alveolar exudate. Although scattered intraalveolar neutrophils are consistently observed in the exudative phase of DAD, dense neutrophil influx suggests concomitant bacterial pneumonia.

The histologic features that allow differentiation of the proliferative phase of DAD from BOOP or UIP are listed in Table 14-1. The clinical setting is extremely helpful in separating these three entities, because DAD is usually associated with an acute fulminant illness, but BOOP and UIP are, respectively, subacute or chronic. A subset of DAD of unknown etiology and corresponding to rapidly progressive pulmonary fibrosis similar to that described by Hamman and Rich is called acute interstitial pneumonia.[24,25] Compared with the clinical course of ARDS as seen, for example, in patients with trauma or sepsis, the duration of respiratory symptoms in patients with acute interstitial pneumonia tends to be more protracted, but the histologic features are virtually identical to the proliferative phase of DAD.

DAD represents a stereotypic response of the lung to injury and is not in itself a clinical diagnosis. After the histologic pattern of DAD is recognized, the determination of the inciting insult can be a formidable task, requiring detailed correlation of clinical events and microbiologic data with the phase of DAD and subtle histologic clues that suggest possible etiologies.

MISCELLANEOUS SYNDROMES OF NONCARDIOGENIC PULMONARY EDEMA

Causes of pulmonary edema that cannot be ascribed to cardiac failure or increased permeability after massive injury to the alveolocapillary membrane are presented in Display 14-2. Some of these syndromes of pulmonary edema can be readily explained by perturbations in the Starling equation or impaired lymphatic clearance. In many, however, the cause of edema formation is multifactorial or unknown.

Fluid overload or decreased plasma oncotic pressure (*e.g.*, hypoalbuminemia) usually do not cause significant pulmonary edema, but they may interact with cardiac failure or alveolar injury to exacerbate edema formation. Some of these miscellaneous disorders of noncardiogenic pulmonary edema are incorrectly listed as examples of ARDS. In contrast to the previously described

TABLE 14-1
Features of Diffuse Alveolar Damage, Bronchiolitis Obliterans
Organizing Pneumonia, and Usual Interstitial Pneumonia

Characteristic	Diffuse Alveolar Damage	Bronchiolitis Obliterans Organizing Pneumonia	Usual Interstitial Pneumonia
Distribution of lesions	Diffuse, solid	Patchy, solid	Diffuse reticulo-nodular
Age of lesions	Uniform	Uniform	Variable
Degree of inflammation	Mild	Moderate to severe	Moderate to severe
Hyaline membranes	Present	Absent	Absent
Organizing fibrin	Extensive	Mild or moderate	Mild
Bronchiolitis obliterans	Minimal	Prominent	Mild
Pneumocyte hyperplasia	Diffuse, atypical	Focal, bland	Diffuse, bland
Fibrosis	Myxoid intraluminal, alveoloseptal	Myxoid intraluminal	Collagenous alveoloseptal

progressive lung injury of ARDS, the syndromes of pulmonary edema in Display 14-2 are usually reversible, do not progress to interstitial fibrosis, and less frequently cause death.[10]

The histopathologic features vary among these disorders, from fibrin-rich pulmonary edema with hyaline membranes as seen in uremia to intraalveolar flooding, alveolar hemorrhage, and capillary congestion resembling cardiogenic edema. Different histologic patterns are probably related to the extent of endothelial injury and complicating factors such as pneumonia, aspiration, or oxygen toxicity. The histopathology of many of these syndromes has been poorly documented because of the low fatality rate. Several specific examples of noncardiogenic edema are discussed in the following sections.

DISPLAY 14-2. CAUSES OF NONCARDIOGENIC PULMONARY EDEMA

Decreased Plasma Oncotic Pressure*

Hypoalbuminemia
Fluid overload
Uremia

Decreased Interstitial Pressure

Lung reexpansion (e.g., pneumothorax, pleural effusion)
Laryngospasm
Hanging (?)

Lymphatic Obstruction

Metastatic neoplasm
Fibrosing mediastinitis

Mechanism Unknown

Neurogenic pulmonary edema
High-altitude pulmonary edema
Tocolytic therapy
Narcotics abuse
Cardiopulmonary bypass
Pulmonary embolism
Lung reperfusion

* Usually acts in concert with other causes to produce pulmonary edema.

High-Altitude Pulmonary Edema

High-altitude pulmonary edema is an uncommon disorder that affects susceptible persons after a rapid transition from low to high altitudes (>2700 m or 9000 ft).[26] Vigorous exercise and cold air exposure are possible precipitating factors. It usually affects young, previously healthy persons and is characterized by dyspnea, nonproductive cough, and diffuse radiographic alveolar infiltrates. The syndrome is relieved by returning to lower altitudes (see Chap. 24).

The mechanism of edema formation is poorly understood but thought to result from a constitutional, exaggerated, pulmonary vasoconstrictive response to hypoxia. Irregular distribution of vasoconstriction may lead to regional overperfusion at high arterial pressure of the nonconstricted (i.e., unprotected) vascular bed.[26] The association of an increased risk of high-altitude pulmonary edema in persons with unilateral absence of the pulmonary artery supports the overperfusion theory.[26] Bronchoalveolar lavage (BAL) studies, however, demonstrate an increased protein concentration and proteins of higher molecular weight than in normal controls. BAL cell counts indicate a significant increase in alveolar macrophages. The pulmonary pathologic features in patients who die of high-altitude pulmonary edema include proteinaceous alveolar edema, hyaline membranes, macrophages, neutrophils, and arterial thromboemboli.[27,28] The findings of BAL and the scant histologic data suggest a component of permeability pulmonary edema. Hypoxia per se is not a significant cause of increased lung capillary permeability in this disorder.[26]

Neurogenic Pulmonary Edema

Pulmonary edema is a recognized complication after a central nervous system (CNS) insult such as epileptic seizures, head trauma, or intracerebral hemorrhage.[29] The symptoms associated with neurogenic pulmonary edema are usually mild and readily reversible; occasionally, pulmonary edema is progressive and causes death. Postmortem studies of sudden death in young epileptics demonstrate moderate to severe pulmonary edema with a marked increase in total lung weight. Histologic features of neurogenic pulmonary edema include homogeneous eosinophilic fluid in
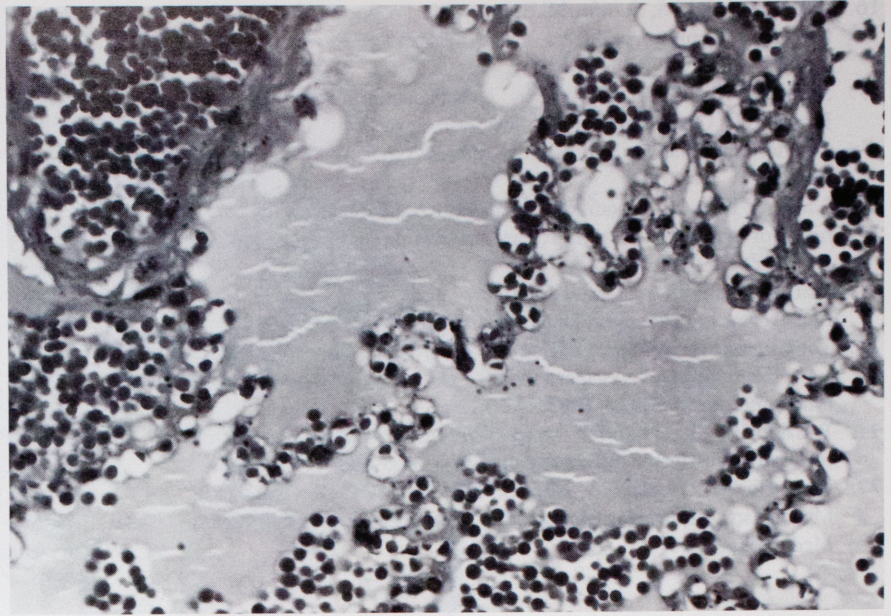
FIGURE 14-16. In a patient with neurogenic pulmonary edema after a fatal gunshot wound to the head, the alveolar capillaries are congested, and alveolar spaces are filled with edema fluid and erythrocytes. (H & E stain; intermediate magnification; courtesy of Carlos Santoscoy, M.D., Cleveland, OH.)

septa and air spaces, severe capillary congestion, and intraalveolar hemorrhage (Fig. 14-16).

The mechanism of edema formation is complex and probably multifactorial. Neurologic insults appear to cause lung capillary permeability and hydrostatic abnormalities through separate mechanisms. Immediately after CNS injury, sympathetic discharge may elicit a transient blast effect of elevated capillary pressure caused by increased venous return to the heart after systemic vasoconstriction. Left ventricular cardiac failure is thought to result from increased venous return, altered ventricular compliance, and systolic overload due to systemic vasoconstriction.[29] Pulmonary venoconstriction, possibly mediated by norepinephrine, acts in concert with cardiac failure to produce pulmonary edema. The net result of these hemodynamic alterations is an increase in pulmonary blood volume and capillary pressure. This is not the total explanation of the syndrome, because the high protein content of the edema fluid suggests a defect in alveolar capillary permeability. The cause of the permeability defect is unknown, but it may be related to stretched interendothelial pores, cell injury as a result of high intracapillary pressure, or the effect of neurohumoral mediators.[29]

Reexpansion Pulmonary Edema

Unilateral pulmonary edema occurs after rapid lung reexpansion after evacuation of a pneumothorax or pleural effusion.[30] The mechanism implicated in the formation of pulmonary edema is sudden negative intrapleural pressure, which pulls fluid from the capillary bed in accordance with the Starling law. Another possible mechanism may be related to loss of surfactant in the chronically collapsed lung.[30] Lung histopathologic characteristics in one case revealed unilaterally increased lung weight, acute pneumonia, and pulmonary edema without hyaline membranes.[30] Rarely, laryngospasm may be complicated by the development of bilateral pulmonary edema.[31] The explanation for pulmonary edema in this situation is decreased intrathoracic pressure caused by inspiratory maneuvers against a closed glottis.

REFERENCES

1. Ashbaugh DG, Bigelow DB, Petty TL, Levine BE. Acute respiratory distress in adults. Lancet 1967;2:319.
2. Katzenstein AA, Bloor CM, Liebow AA. Diffuse alveolar damage: the role of oxygen, shock and related factors. Am J Pathol 1976;85:210.
3. Burford TH, Burbank B. Traumatic wet lung. J Thorac Surg 1945; 14:415.
4. Moon VH. The pathology of secondary shock. Am J Pathol 1948; 25:235.
5. Jenkins MT, Jones RF, Wilson B, Moyer CA. Congestive atelectasis—a complication of the intravenous infusion of fluids. Ann Surg 1950; 132:327.
6. Nash G, Blennerhasset JB, Pontoppidan H. Pulmonary lesions associated with oxygen therapy and artificial ventilation. N Engl J Med 1967;276:368.
7. Bachofen M, Weibel ER. Alterations of the gas exchange apparatus in adult respiratory insufficiency associated with septicemia. Am Rev Respir Dis 1977;116:589.
8. Pratt PC, Vollmer RT, Shelburne JD, Crapo JD. Pulmonary morphology in a multihospital collaborative extracorporeal membrane oxygenation project. I. Light microscopy. Am J Pathol 95;1979:191.
9. Jones R, Reid LM, Zapol WM, Tomashefski JF Jr, Kirton OC, Kobayashi K. Pulmonary vascular pathology. Human and experimental studies. In: Zapol WM, Falke KJ, eds. Acute respiratory failure. New York: Marcel Dekker, 1985:23.
10. Hudson LD. Causes of the adult respiratory distress syndrome—clinical recognition. Clin Chest Med 1982;3:195.
11. Greene R. Adult respiratory distress syndrome: acute alveolar damage. Radiology 1987;163:57.
12. Tomashefski JF Jr. Pulmonary pathology of the adult respiratory distress syndrome. Clin Chest Med 1990;11:593.
13. Fukuda Y, Ishizaki M, Masuda Y, Kimura G, Kawanami O, Masugi Y. The role of intraalveolar fibrosis in the process of pulmonary structural remodeling in patients with diffuse alveolar damage. Am J Pathol 1987;126:171.
14. Churg A, Golden J, Fligiel S, Hogg JC. Bronchopulmonary dysplasia in the adult. Am Rev Respir Dis 1983;127:117.
15. Zapol WM, Trelstad RL, Coffey JW, Tsai I, Salvador RA. Pulmonary fibrosis in severe acute respiratory failure. Am Rev Respir Dis 1979; 119:547.

16. Lakshminarayan S, Stanford RE, Petty TL. Prognosis after recovery from adult respiratory distress syndrome. Am Rev Respir Dis 1976; 113:7.

17. Suchyta MR, Elliott CG, Colby T, Rasmusson BY, Morris AH, Jensen RL. Open lung biopsy does not correlate with pulmonary function after the adult respiratory distress syndrome. Chest 1991; 99:1232.

18. Lamy M, Fallat RJ, Koeniger E, et al. Pathologic features and mechanisms of hypoxemia in adult respiratory distress syndrome. Am Rev Respir Dis 1976;114:267.

19. Pratt PC. Pathology of adult respiratory distress syndrome: implications regarding therapy. Semin Respir Med 1982;4:79.

20. Tomashefski JF Jr, Davies P, Boggis C, Greene R, Zapol WM, Reid LM. The pulmonary vascular lesions of the adult respiratory distress syndrome. Am J Pathol 1983;112:112.

21. Rinaldo JE, Christman JW. Mechanisms and mediators of the adult respiratory distress syndrome. Clin Chest Med 1990;11:621.

22. Marinelli WA, Henke CA, Harmon KR, Hertz MI, Bitterman PB. Mechanisms of alveolar fibrosis after acute lung injury. Clin Chest Med 1990;11:657.

23. Weiss SJ. Tissue destruction by neutrophils. N Engl J Med 1989; 320:365.

24. Katzenstein AA, Myers JL, Mazur MT. Acute interstitial pneumonia: a clinicopathologic, ultrastructural and cell kinetic study. Am J Surg Pathol 1986;10:256.

25. Olson J, Colby TV, Elliott CG. Hamman-Rich syndrome revisited. Mayo Clin Proc 1990;65:1538.

26. Schoene RB. Pulmonary edema at high altitude: review, pathophysiology, and update. Clin Chest Med 1985;6:491.

27. Arias-Stella J, Kruger H. Pathology of high altitude pulmonary edema. Arch Pathol 1963;76:147.

28. Dickinson J, Heath D, Gosney J, Williams D. Altitude related deaths in seven trekkers in the Himalayas. Thorax 1983;38:646.

29. Colice GL, Matthay MA, Bass E, Matthay RA. Neurogenic pulmonary edema. Am Rev Respir Dis 1984;130:941.

30. Sautter RD, Dreher WH, MacIndoe JH, Myers WO, Magnin GE. Fatal pulmonary edema and pneumonitis after re-expansion of chronic pneumothorax. Chest 1971;60:399.

31. Jackson FN, Rowland V, Corssen G. Laryngospasm-induced pulmonary edema. Chest 1980;78:819.
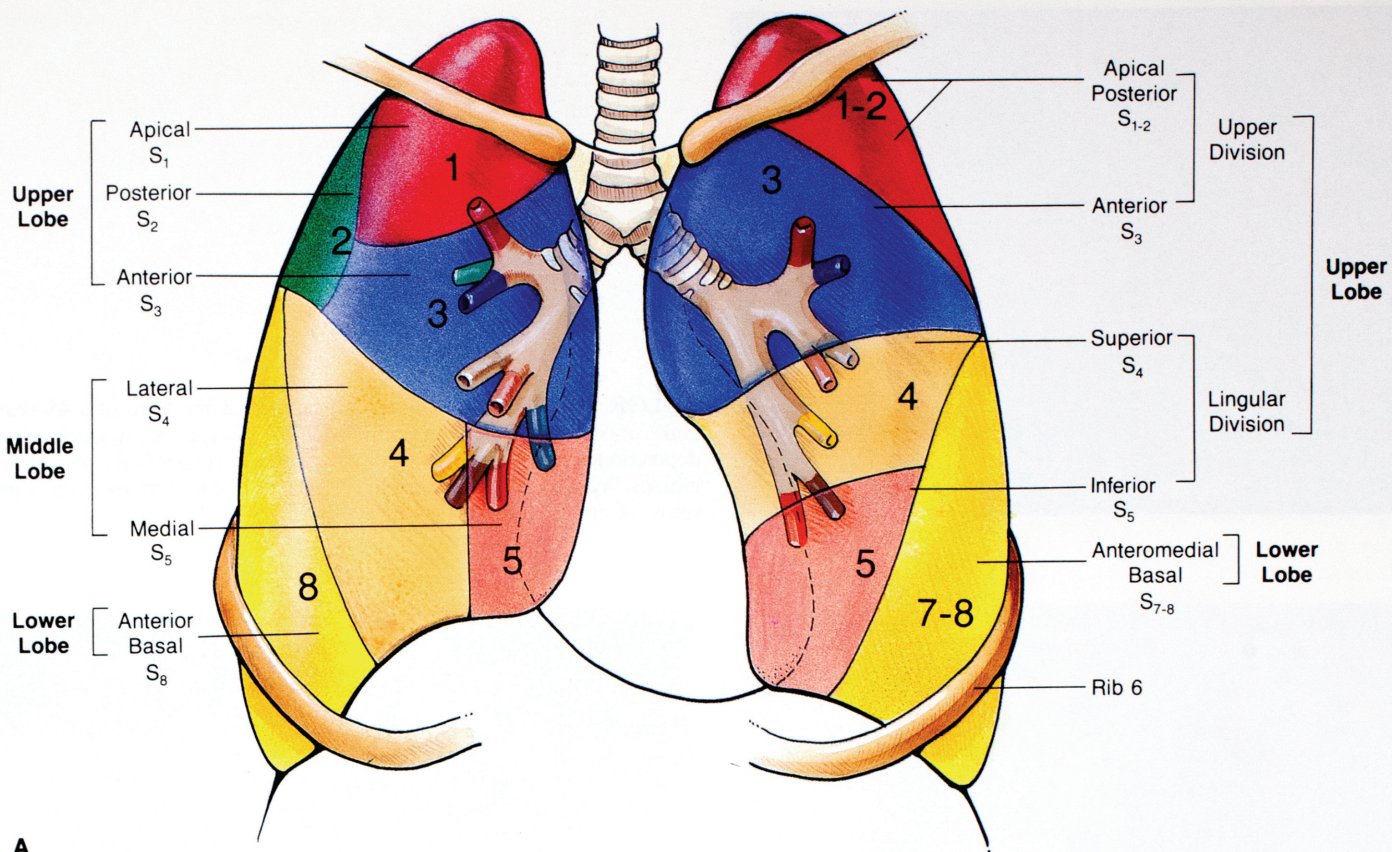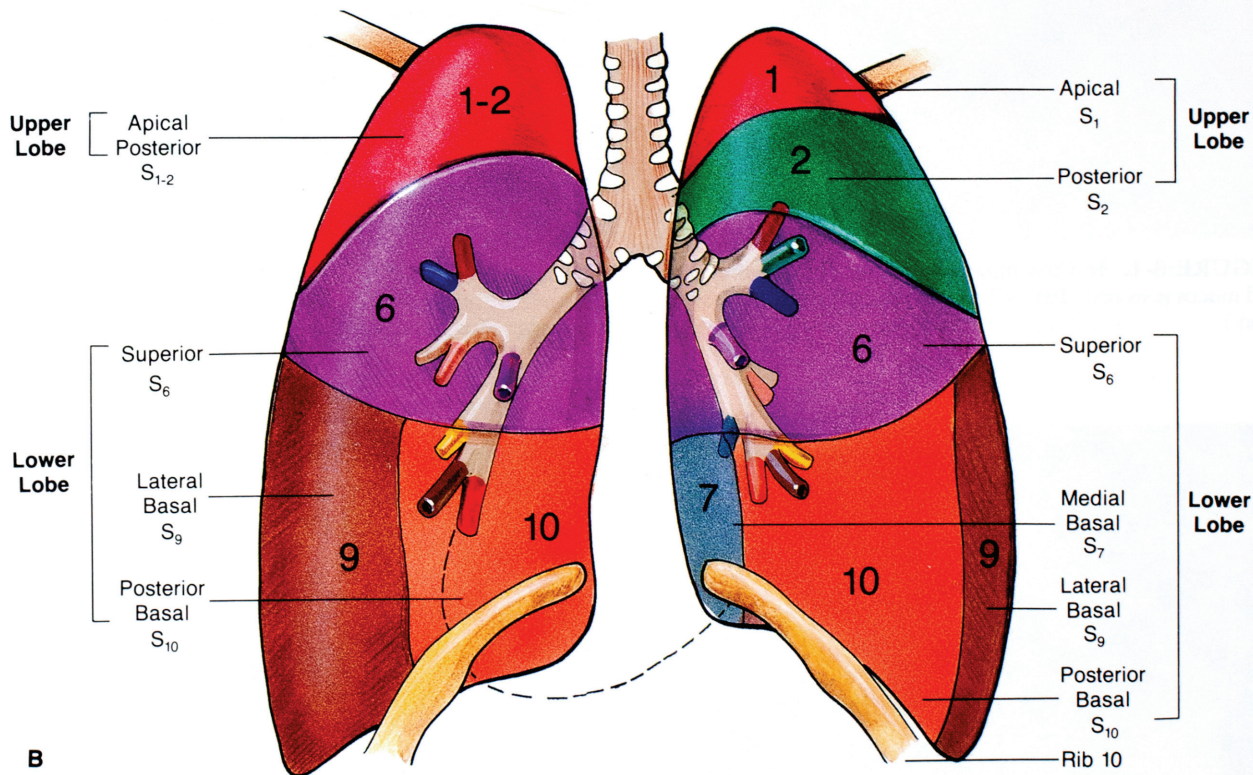
COLOR FIGURE 1-1. (**A**) Anterior and (**B**) posterior views of the human lung demonstrate the bronchopulmonary segments. The number of segments can vary from 18 to 20, depending on whether the apical and posterior segments of the upper lobe and the anterior and medial basal segments of the lower lobe in the left lung are fused. The right lung is divided into 10 segments: three in the upper lobe, two in the middle lobe, and 5 in the lower lobe. The left lung is likewise divided into 10 segments. The left upper lobe is equivalent to the upper and middle lobes of the right lung, with an upper division equivalent to the right upper lobe, and a lower or lingular division is comparable to the right middle lobe. (Copyrighted by the University of Texas Health Science Center at San Antonio, 1993.)

COLOR FIGURE 1-2. Gross appearance of the lung of a 45-year-old male smoker who died of nonpulmonary disease. Anthracotic pigment deposition demarcates polyhedral spaces corresponding to secondary lobules. White tracts at the periphery of the secondary lobules are pulmonary veins. (Contributed by the editor.)
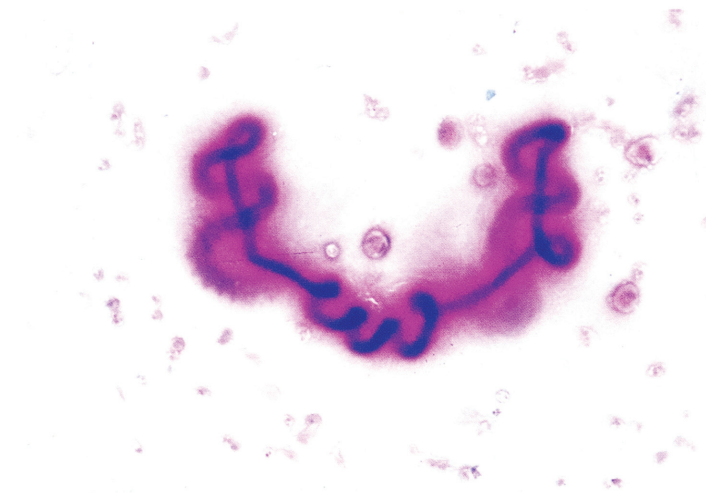
COLOR FIGURE 3-1. In Curschmann spiral, the dark-staining core of inspissated mucus is surrounded by lighter mucus. (Papanicolaou stain; oil immersion.)
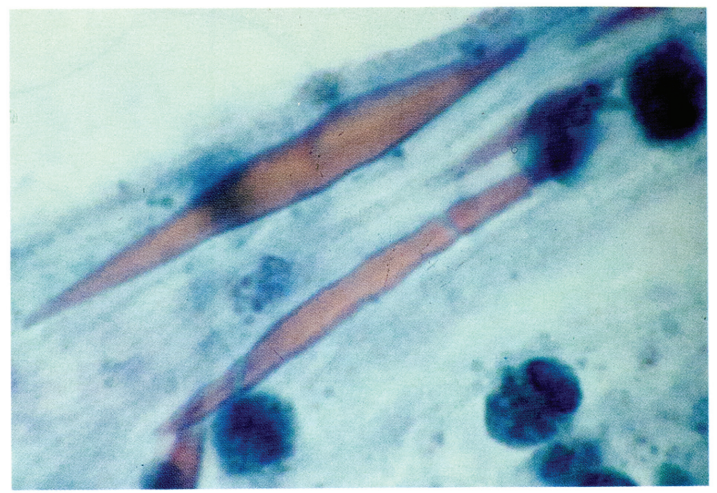
COLOR FIGURE 3-2. Charcot-Leyden crystals from an asthmatic patient have an elongated shape with pointed extremities. (Toluidine blue stain; wet film; oil immersion.)
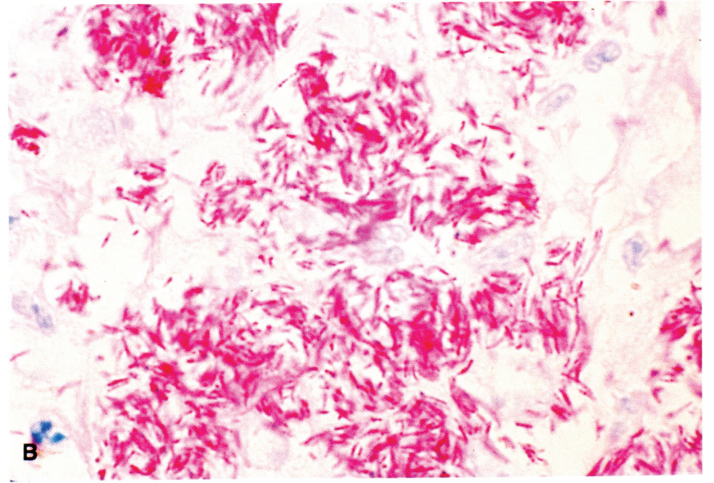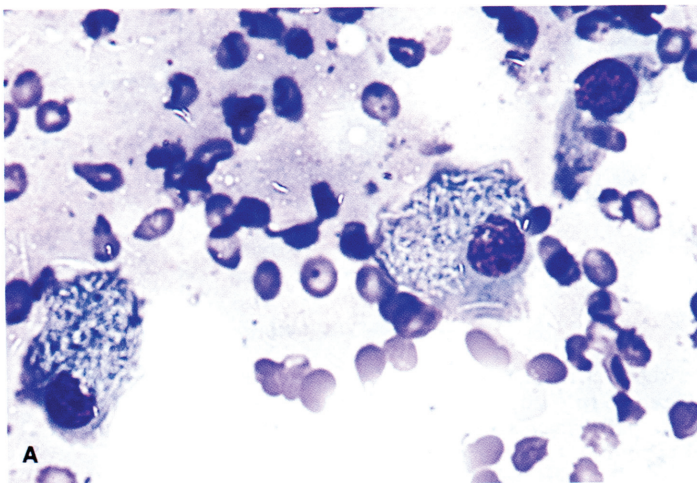
COLOR FIGURE 3-3. (A) Macrophage with a negative image of needle like bacilli crowding the cytoplasm. (Papanicoloau stain; oil immersion.) (B) An acid-fast stain shows a large number of bacilli that correspond to the negative spaces in A. (Kinyoun stain; oil immersion.)
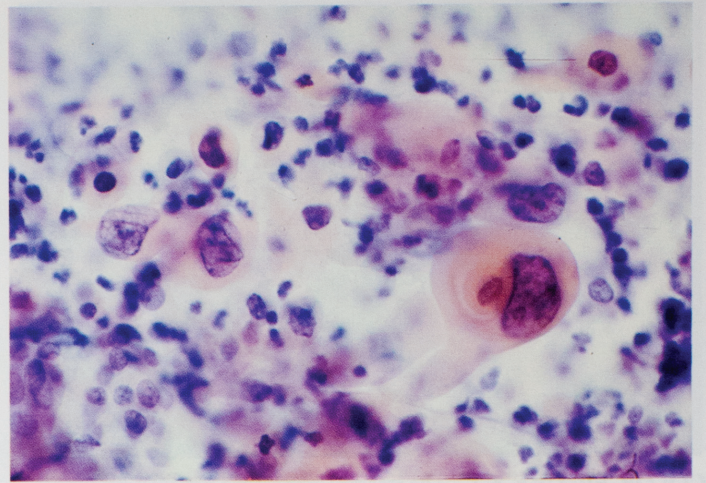
COLOR FIGURE 3-4. This squamous cell carcinoma contains intensely eosinophilic malignant keratinocytes and large numbers of neutrophils. (Papanicolaou stain; oil immersion.)
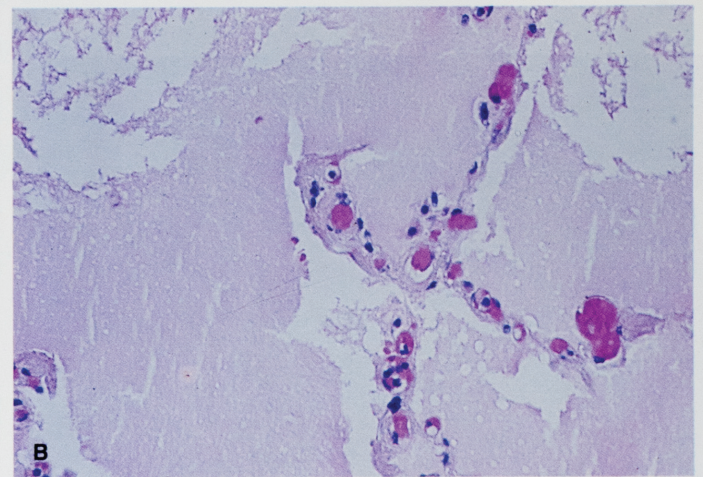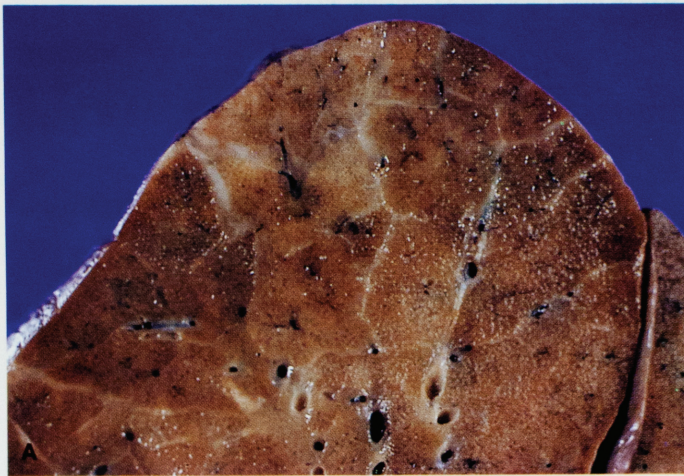
COLOR FIGURE 5-1. (**A**) Gross appearance of a lung with cardiogenic pulmonary edema from a middle-aged woman with mitral valvular disease. After formalin perfusion, the lungs were firm and shiny. (**B**) In a microscopic section from the same patient, pink edema fluid fills the alveoli. (H & E stain; intermediate magnification.)
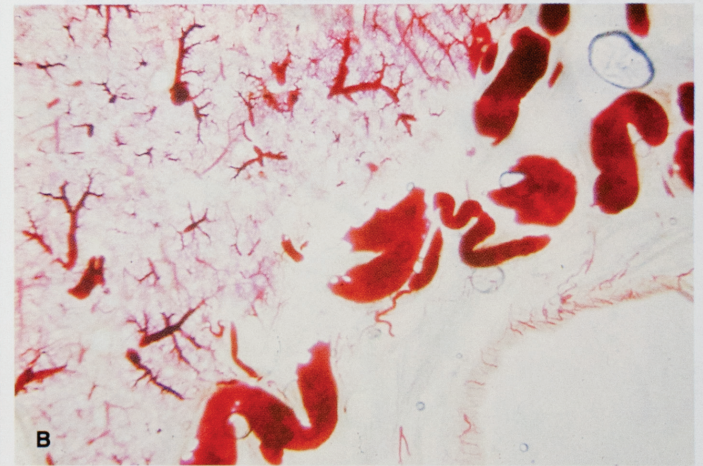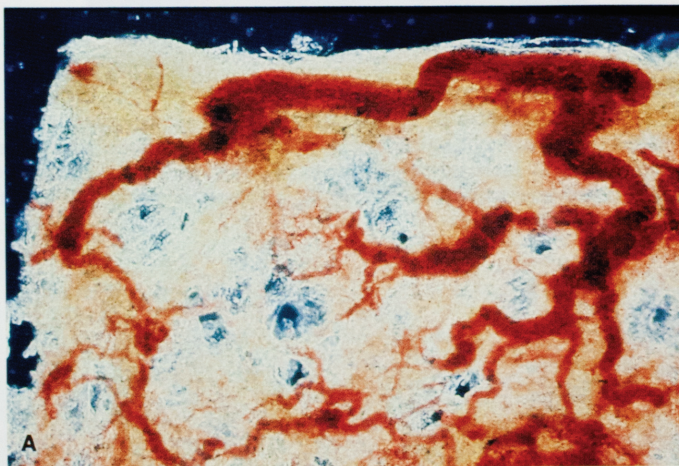
COLOR FIGURE 5-2. Bronchial artery collateral vessels injected in a dog with severe pulmonary hypertension following a systemic-pulmonary arterial anastomosis.(**A**) View of the pleura. (**B**) Wall of bronchus and adjacent lung tissue. (Panoramic view; viewed through a dissecting microscope.) All the vessels present were injected from the aorta. (From Saldana ME, Harley RA, Liebow AA, Covington CB. Experimental extreme pulmonary hypertension and vascular disease in relation to polycythemia. Am J Pathol 1968;52:935.)
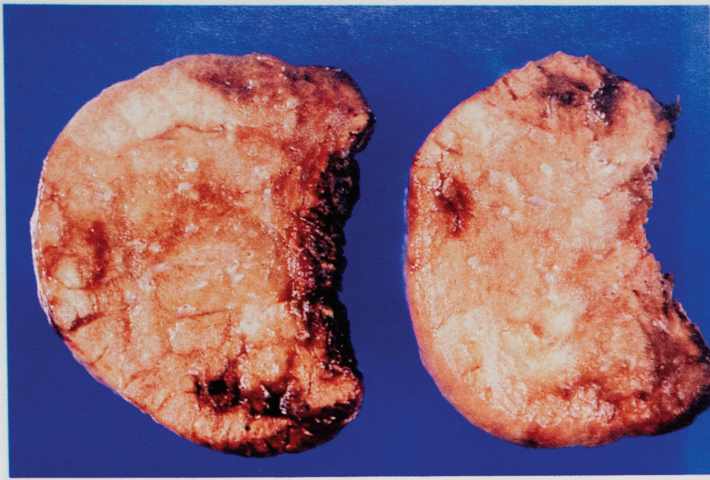
COLOR FIGURE 8-1. The resected lobe from a patient with congenital lobar emphysema is soft and well aerated after formalin fixation (see Fig. 8-2). (Courtesy of Daphne deMello, M.D., St. Louis, MO.)
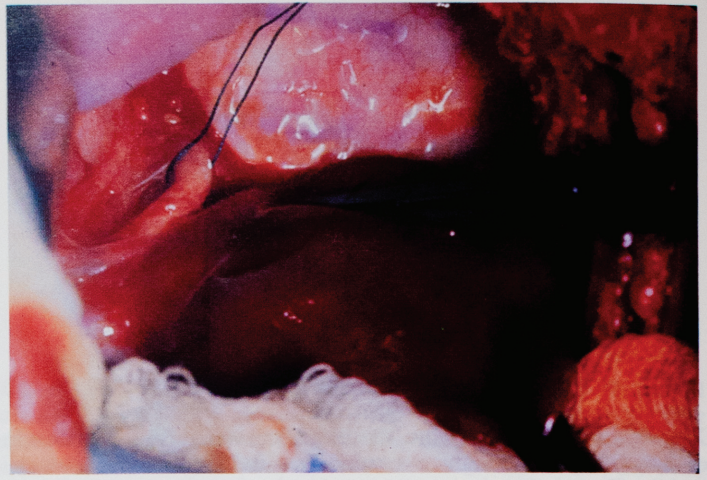
COLOR FIGURE 8-2. A left, supradiaphragmatic, deeply red mass represents extralobar sequestration (*i.e.*, Rokitansky lobe). A thread of black silk identifies the systemic artery supplying the sequestration. (Courtesy of Juan Payser, M.D., Miami, FL.)
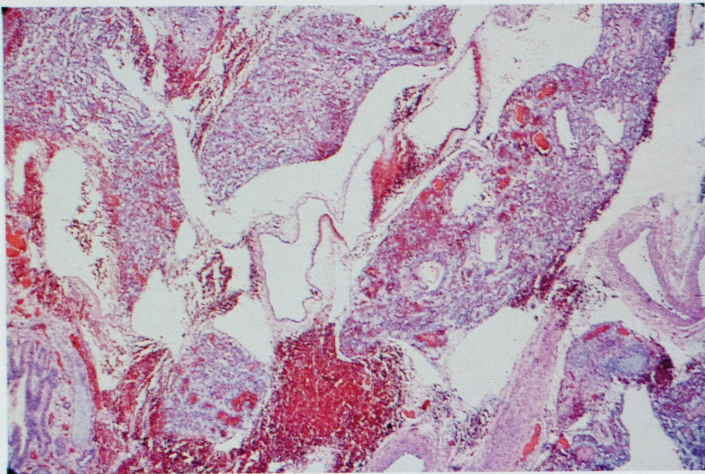
COLOR FIGURE 9-1. A microscopic view of lung tissue from a newborn with congenital pulmonary lymphangiectasis associated with total anomalous pulmonary venous return. Markedly dilated lymphatic vessels between secondary lobules produce atelectasis of alveolar tissue and reduce lung compliance. (Trichrome stain; low magnification; courtesy of Daphne deMello, M.D., St. Louis, MO.)
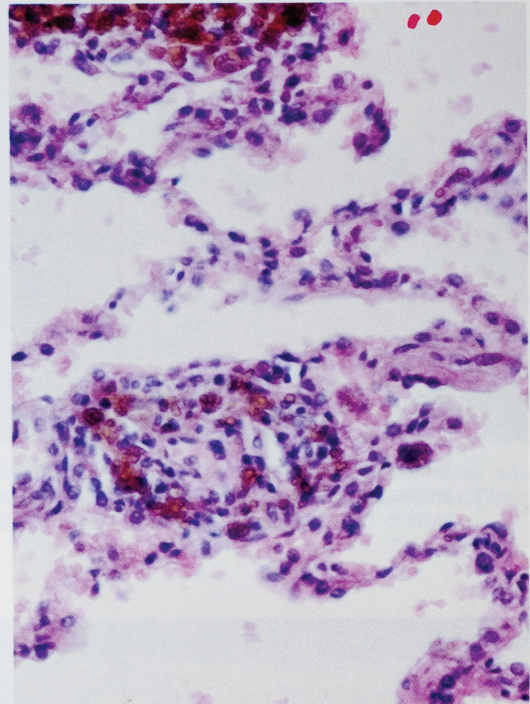
COLOR FIGURE 9-3. A microscopic view of a lung biopsy specimen shows what probably represents an early stage of primary pulmonary hemosiderosis. Interstitial hemosiderin deposits, and hypercellularity of alveolar septa are present. (H & E stain; intermediate magnification; contributed by the editor.)
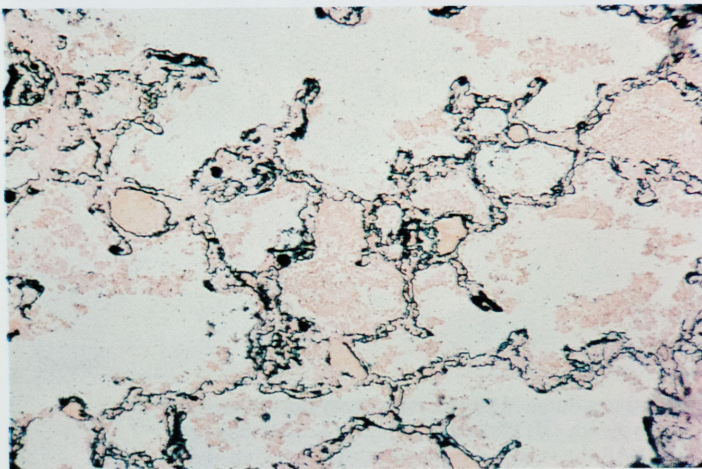
COLOR FIGURE 9-2. Alveolar tissue stained by the von Kossa method reveals widespread, alveolar septal deposits of calcium in a patient with septal and stromal calcinosis. (Low magnification.)

COLOR FIGURE 9-4. Massive iron deposition in alveolar tissue characterizes pulmonary hemosiderosis in a 16-year-old girl with thalassemia major. (Perls' Prussian blue test; low magnification.)
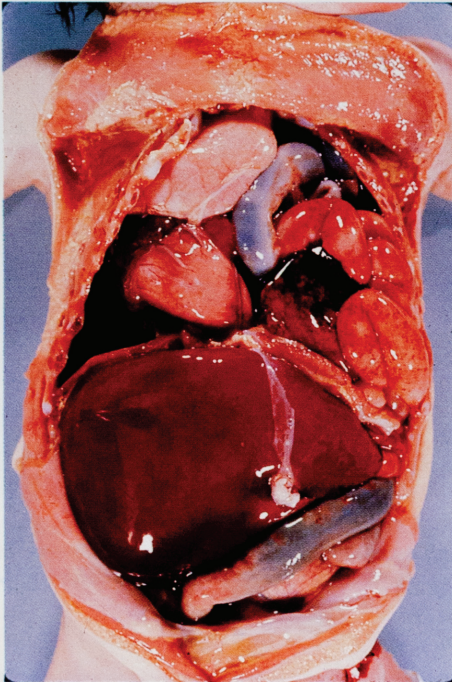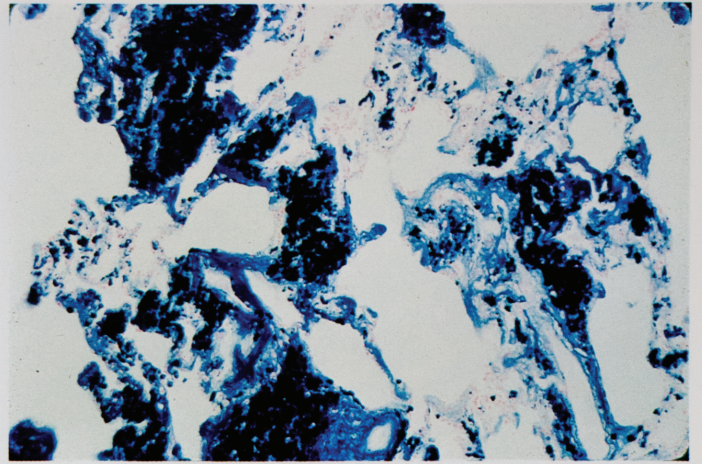
COLOR FIGURE 10-1. A large, left diaphragmatic hernia caused the death of this newborn infant. At necropsy, the left chest cavity was filled with abdominal visceral contents (see Fig. 10-2). (Courtesy of Juan Payser, M.D., Miami, FL.)
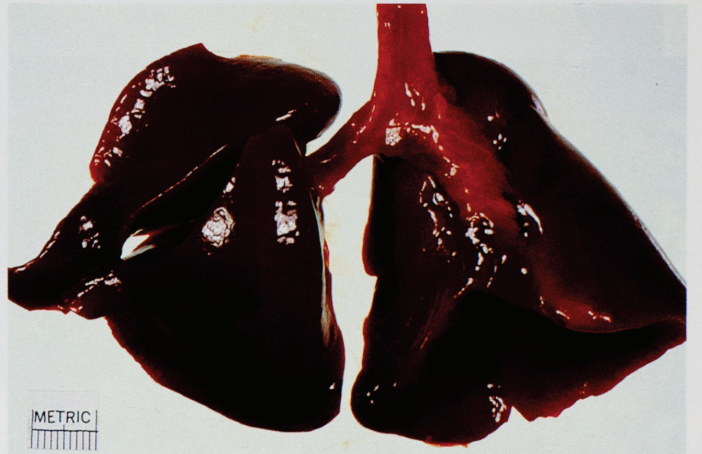

COLOR FIGURE 11-1. Gross appearance of lung specimen in a patient with hyaline membrane disease, stage II. The lungs are deeply congested and rubbery firm, resembling liver tissue.
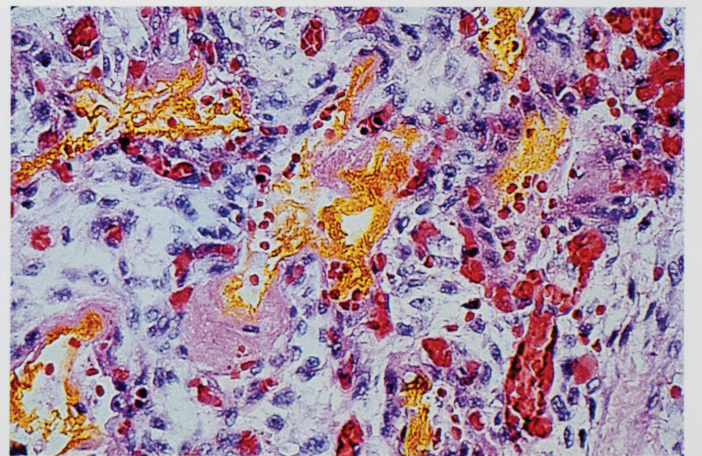
COLOR FIGURE 11-2. An admixture of yellow and pink hyaline membranes in alveolar tissue. Yellow membranes were a common finding in autopsy material a few decades ago. The reasons for their frequency of occurrence in the past and their present rarity have not been clarified. (H & E stain; intermediate magnification; contributed by the editor.)
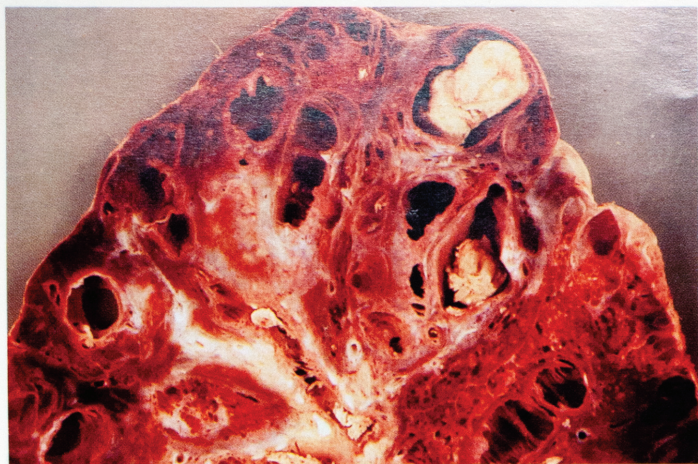
COLOR FIGURE 11-3. Right pneumonectomy specimen from a 22-year-old woman with cystic fibrosis of the pancreas. Note the presence of extensive bronchiectasis with mucus plugging, preferentially affecting the upper lobe. (Contributed by the editor.)
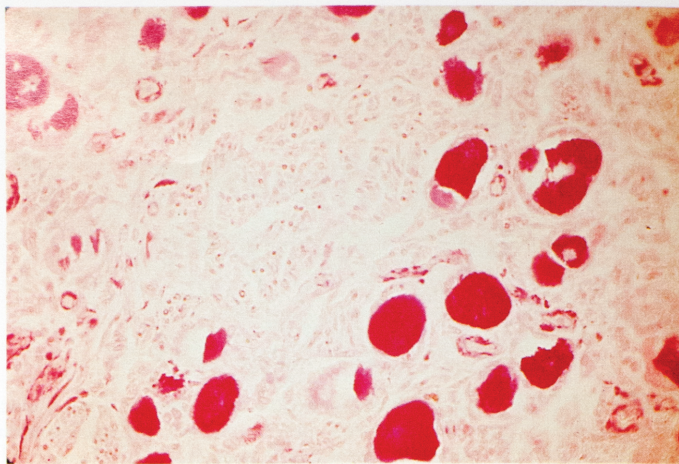

COLOR FIGURE 12-1. Strong PAS-positivity of neurons of a sympathetic ganglion occurs in a patient with Fabry disease. (Low magnification; courtesy of Joyce Bruce, M.D., Miami, FL.)
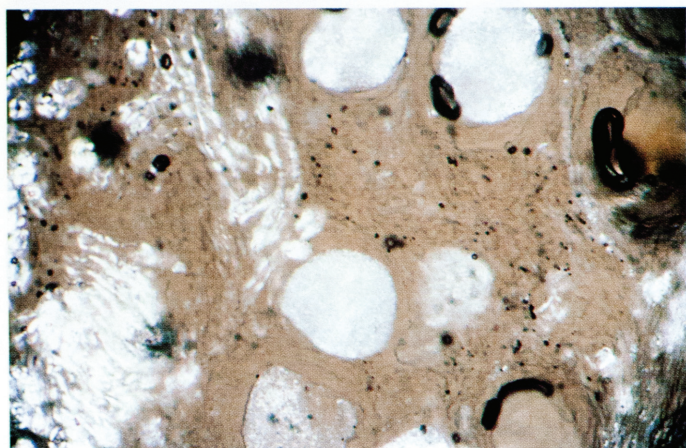

COLOR FIGURE 12-2. Strong birefringency of neurons of a sympathetic ganglion is also present in the patient with Fabry disease in Color Figure 12-1. (H & E stain; intermediate magnification; courtesy of Joyce Bruce, M.D., Miami, FL.)
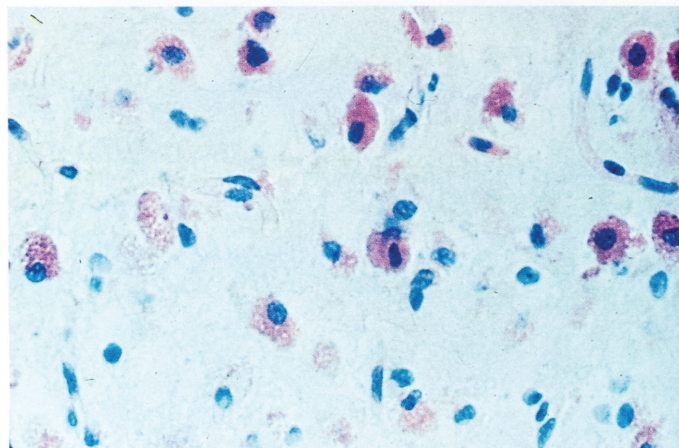
COLOR FIGURE 12-3. PAS-positivity occurs as the result of the presence of glycogen in the cells of a patient with Pompe disease. (Intermediate magnification; courtesy of Michael Norenberg, M.D., Miami, FL.)
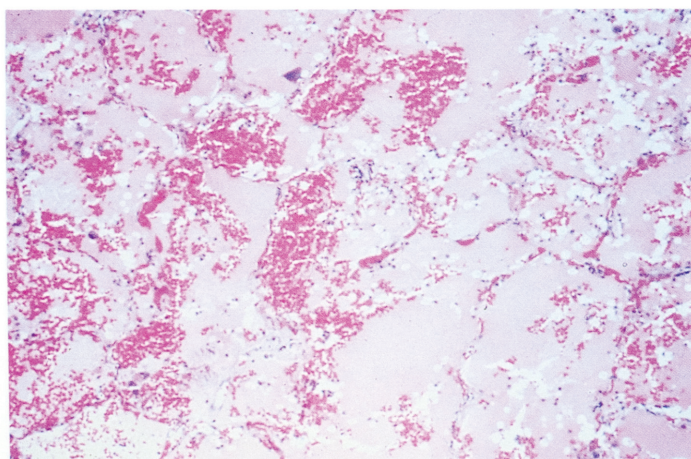

COLOR FIGURE 13-1. In cardiogenic pulmonary edema, edema fluid passes into the alveoli. Depending on its protein concentration, the fluid is either transparent or faintly stained. Congestion is evident; many erythrocytes lie freely in the alveoli and pack the capillaries in the alveolar walls. (H & E stain, low magnification; contributed by the editor.)
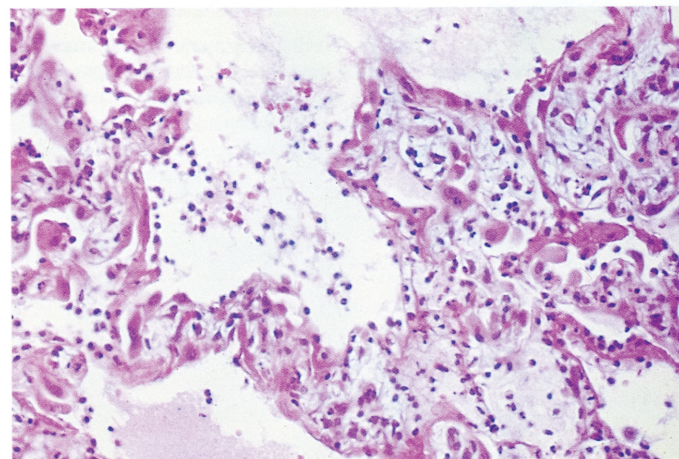
COLOR FIGURE 13-2. Permeability pulmonary edema in uremia shows heavy fibrinous intraalveolar edema with hyaline membranes and acute inflammatory cells. (H & E stain; low magnification; contributed by the editor.)
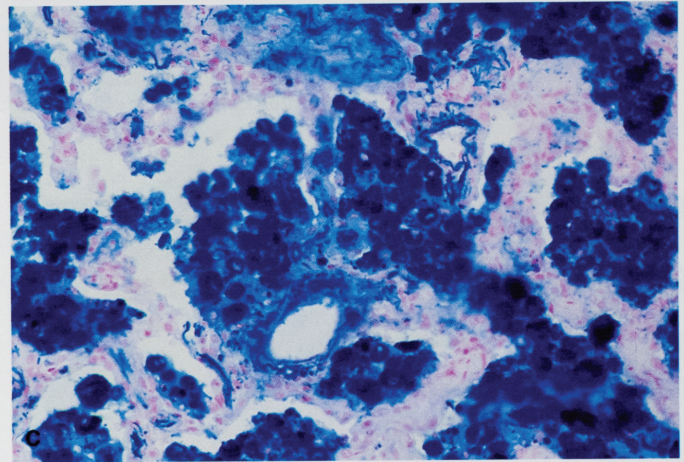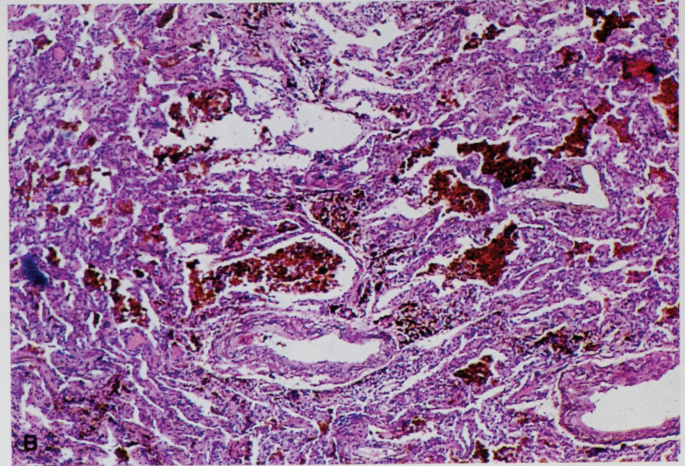
COLOR FIGURE 13-3. Lung specimens from a patient with secondary hemosiderosis caused by cardiomyopathy. (**A**) Rusty discoloration of the lungs is characteristic of this condition (*i.e.*, brown induration). (**B**) A microscopic view shows numerous collections of hemosiderin-laden macrophages in the alveolar spaces. (H & E stain; low magnification.) (**C**) An iron stain of alveolar tissue in same patient is strikingly positive. (Prussian blue iron stain; intermediate magnification; contributed by the editor.)


COLOR FIGURE 14-1. In the exudative phase of diffuse alveolar damage, the parenchymal surface is diffusely consolidated with an airless, liverlike appearance. There is also confluent pleural hemorrhage.
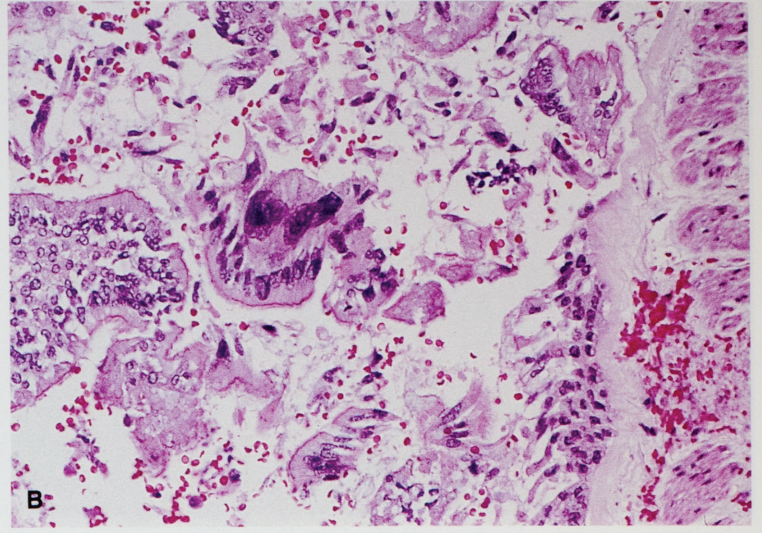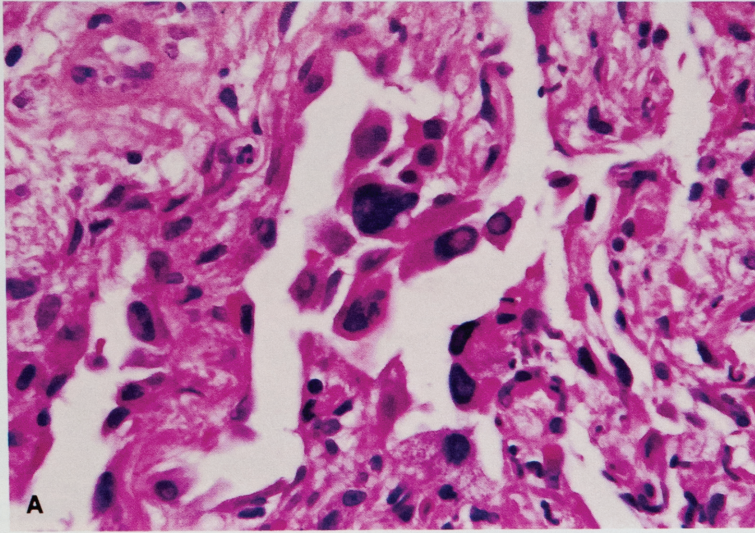
COLOR FIGURE 16-1. Bleomycin-associated patchy interstitial inflammation and fibrosis. (**A**) Hyperplasia of the alveolar lining cells occurs with marked atypia, pleomorphism, hyperchromasia, and lack of mitotic figures. These cells are associated with interstitial fibrosis and mild inflammation. (H & E stain; intermediate magnification.) (**B**) Similar atypia is found in bronchial lining cells. (H & E stain; low magnification.)
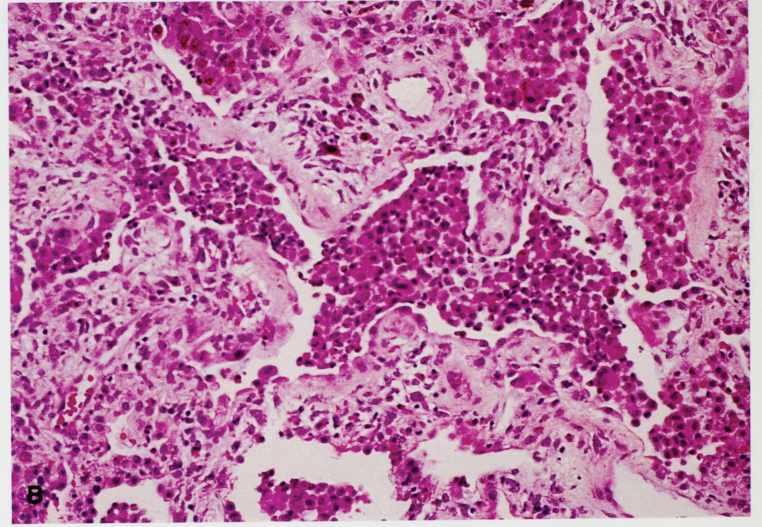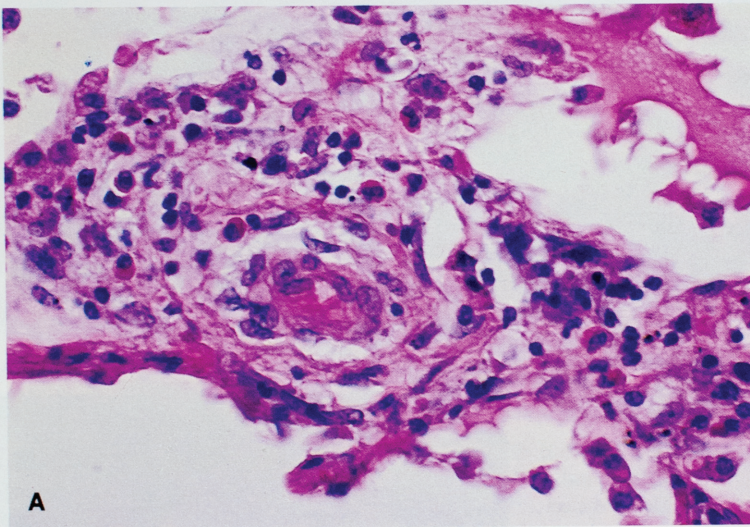
COLOR FIGURE 16-2. Eosinophilic pneumonia. (**A**) A high-power view of a lung biopsy specimen in a patient taking sulfonamide demonstrates a prominent number of eosinophils in the interstitial inflammatory infiltrate (see Fig. 16-4). (H & E stain; intermediate magnification.) (**B**) Chronic eosinophilic pneumonia with alveoli filled by histiocytes and eosinophils is typical. The interstitium also shows inflammation and fibrosis. The patient developed bilateral peripheral infiltrates while taking bleomycin for lymphoma; some of the infiltrates appeared nodular, and the clinical differential diagnosis included recurrent lymphoma. (H & E stain; low magnification.)